Sequence stratigraphy of experimental strata under known conditions of differential subsidence and variable base level

John Martin, Chris Paola, Vitor Abreu, Jack Neal, and Ben Sheets

ABSTRACT

Sequence stratigraphy has been applied from reservoir to continental scales, providing a scale-independent model for predicting the spatial arrangement of depositional elements. We examine experimental strata deposited in the Experimental EarthScape facility at St. Anthony Falls Laboratory, focusing on stratigraphic surfaces defined by discordant contact geometries, surfaces analogous to those delineated in the original work on seismic sequence stratigraphy. In this controlled setting, we directly evaluate critical sequence-stratigraphic issues, such as stratigraphic horizon development and time significance, as well as the internal geometry and migration of the bounded strata against the known boundary conditions and depositional history.

Four key stratigraphic disconformities defined by marine downlap, marine onlap, fluvial erosion, and fluvial onlap are mapped and vary greatly in their relative degree of time transgression. Marine onlap and downlap contacts closely parallel topographic surfaces (time surfaces) and, prior to burial, approximate the instantaneous offshore topography. These stratal-bounding surfaces are also robust stratigraphic signals of relative base-level fall and rise, respectively. Marine onlap surfaces are of special interest. They tend to be the best preserved discordance, where widespread, allogenic-based onlap surfaces subdivide otherwise amalgamated depositional cycles amidst cryptic stacks of marine foresets; however, local, autogenic-based marine

Manuscript received May 23, 2008; provisional acceptance July 16, 2008; revised manuscript received November 4, 2008; final acceptance December 11, 2008.
DOI:10.1306/12110808057

AUTHORS

JOHN MARTIN ~ *St. Anthony Falls Laboratory and Department of Geology and Geophysics, University of Minnesota, Minneapolis, Minnesota; present address: Integrated Reservoir Performance Prediction, ExxonMobil Upstream Research Company, P.O. Box 2189, Houston, Texas 77252-2189; john.m.martin@exxonmobil.com*

John M. Martin is presently at ExxonMobil Upstream Research Company, where his research interests are in geomorphology and the details of stratigraphic accumulation from a variety of depositional environments. He earned his Ph.D. from the University of Minnesota, Minneapolis, where much of his work was centered at St. Anthony Falls Laboratory.

CHRIS PAOLA ~ *St. Anthony Falls Laboratory and Department of Geology and Geophysics, University of Minnesota, Minneapolis, Minnesota*

Chris Paola is a professor in the Department of Geology and Geophysics, University of Minnesota, Minneapolis, and does research at St. Anthony Falls Laboratory. His research interests are in physical sedimentary geology and stratigraphy, especially the dynamics of channelized systems. He received his B.S. degree in environmental geology from Lehigh University, his M.S. degree in applied sedimentology from the University of Reading, and his D.S. degree in marine geology from Massachusetts Institute of Technology/Woods Hole Oceanographic Institution Joint Program in Oceanography.

VITOR ABREU ~ *ExxonMobil Exploration Company, Houston, Texas*

Vitor Abreu received his Ph.D. from Rice University and is presently an ExxonMobil stratigraphy coordinator. He is also an adjunct professor at Rice University, teaching sequence stratigraphy and has published several articles and given numerous talks and seminars within industry and academia. He was the recipient of the Jules Braunstein Memorial Award (2002 AAPG Annual Meeting) and is currently an AAPG distinguished instructor.

JACK NEAL ~ *ExxonMobil Exploration Company, Houston, Texas*

Jack E. Neal received his B.S. degree from the University of Tulsa and his Ph.D. from Rice

University. His interests are seismic and sequence stratigraphy, structure-stratigraphic interaction, paleoclimate, and hydrocarbon systems. He has published on northwestern Europe sequence stratigraphy, graphic correlation, and lacustrine sequence stratigraphy. He has worked globally in research, exploration, development, and production assignments with Exxon and ExxonMobil since 1994.

BEN SHEETS ~ *ExxonMobil Upstream Research Company, Houston, Texas; present address: School of Oceanography, University of Washington, Seattle, Washington*

Ben Sheets is an assistant professor of marine geology and geophysics in the School of Oceanography at the University of Washington, Seattle. He earned his B.A. degree from Carleton College and his Ph.D. from the University of Minnesota, Minneapolis. His research involves processes, geomorphology, and stratigraphy in a variety of coastal and submarine sedimentary systems.

ACKNOWLEDGEMENTS

This work was supported by the National Science Foundation via the National Center for Earth-surface Dynamics under agreement EAR-0120914. Additional support was provided by the St. Anthony Falls Industrial Consortium, including Anadarko; Chevron; ConocoPhillips; ExxonMobil; and Japan Oil, Gas and Metals National Corporation (JOGMEC). Seismic data analysis was performed with the Kingdom Software, courtesy of Seismic Micro-Technology. We are indebted to the engineers and technical staff at St. Anthony Falls Laboratory, notably Jim Mullin, Chris Ellis, and Dick Christopher, whose dedication and expertise make experimental basin filling possible. We are grateful for thoughtful, comprehensive reviews by Kevin Bohacs, Ashton Embry, and an anonymous reviewer, which considerably improved this manuscript. We also thank David Mohrig, Tony Rukel, John Van Wagoner and Roger Bloch for many insightful discussions that pertain to this work.

onlap discordances are present throughout the fill. A critical distinguishing feature of allogenic onlap is the greater lateral persistence of the discordance. Surfaces defined by subaerial erosional truncation and fluvial onlap do not have geomorphic equivalence because channel processes continually modify the surface as the stratigraphic horizons are forming. Hence, they are strongly time transgressive. Last, the stacking arrangement of the preserved bounded strata is found to be a good time-averaged representation of the mass-balance history.

INTRODUCTION

Seismic sequence stratigraphy is widely used to subdivide the stratigraphic record into unconformity-bounded units (Mitchum et al., 1977a). Its predictive power arises from assumptions concerning the development of sequence-bounding unconformities (and their correlative conformities)—surfaces thought to entirely separate sequences in time—permitting large-scale chronostratigraphic correlation based on stratal contact geometries (Mitchum et al., 1977a; Haq et al., 1987; Posamentier et al., 1988; Van Wagoner et al., 1990). Several sequence-stratigraphic models have been proposed (Nystuen, 1998; Catuneanu, 2002), including the depositional sequence model (e.g., Vail et al., 1977; Posamentier and Vail, 1988; Van Wagoner et al., 1988, 1990), the genetic stratigraphic sequence model (Galloway, 1989), the transgressive-regressive sequence model (Embry, 1993; 2003), and the forced regression sequence model (Hunt and Tucker, 1992; Helland-Hansen and Gjelberg, 1994). Although the details surrounding their development and differences are beyond the scope of this work, these various models all recognize stratigraphic surfaces defined by stratal discordances originally outlined by Mitchum et al. (1977a) as critical elements in interpretation (Figure 1). The models vary in which surfaces they recognize and in the theoretical and applied value they assign to these stratigraphic horizons, leading to emphasis on certain horizons over others (depending on the model of choice). Consequently, different methods for classifying sequence-stratigraphic units for the same stratigraphic succession exist. Sequence-stratigraphic models also incorporate and rely on conformable surfaces to varying degrees. Here, however, we focus on the primary discordant surfaces because their production is mostly independent of scale and sediment type (e.g., Posamentier et al., 1992).

Quantitative sequence-stratigraphic models, which couple sediment mass balance with allogenic forcing mechanisms,

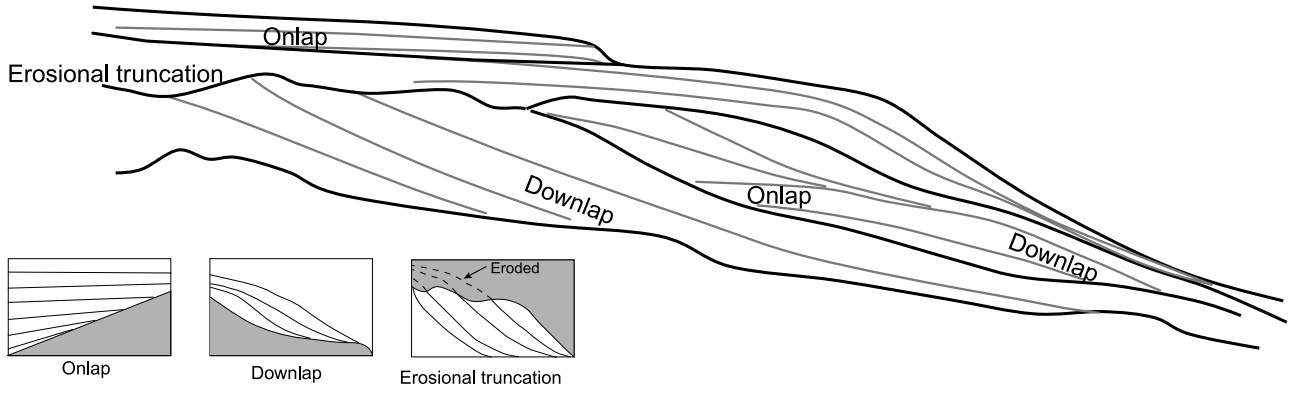

Figure 1. Discordant stratal contact geometries. Illustrations are based on Mitchum et al. (1977a).

have begun to shed light on the timing and partitioning of sediment to sequences (Kendall et al., 1991; Lawrence, 1994; Cross and Lessenger, 1998; Perlmutter et al., 1998). The next step in developing quantitative sequence stratigraphy requires combining careful measurement of the time and space development of stratigraphic horizons with sediment mass partitioning within the stratal packages they bound, similar in spirit to time stratigraphy of Wheeler (1958). Our aim in this article is to do this using a stratigraphic experiment for which we know the basin-fill history and have a complete three-dimensional (3-D) stratigraphic record (e.g., Paola et al., 2001). Specifically, we intend to (1) quantify the timing and development of stratigraphic horizons that underpin much of modern sequence stratigraphy, and (2) measure how these horizons are linked to mass partitioning in the associated deposits. Both are aims for which a complete, mass-balanced data set produced under controlled conditions provides unique insight. In particular, the experimental data set allows us to document when and how primary stratigraphic horizons form under forcing conditions similar to those of the original conceptual depositional sequence models (e.g., Vail et al., 1977; Jervey, 1988; Posamentier and Vail, 1988).

THE STRENGTHS AND LIMITATIONS OF EXPERIMENTAL MODELING

The results we describe below are of an experimental basin fill, which provides a novel environment to explore and quantify linkages between surface processes and subsurface architecture. In fact, given that the boundary conditions can be controlled, surface topography carefully monitored, and internal stratigraphy sectioned almost completely to produce 3-D stratigraphy of a mass-conserved basin fill, we can argue that experiments offer a view of stratigraphic accumulation unavailable from the field (Paola et al., 2001; Van Heijst and Postma, 2001; Sheets et al., 2002; Hickson et al., 2005). These constraints on basin filling cannot be overstated if for no other reason than the resulting data sets serve as both a resource for developing quantitative techniques and a test for prediction, together generating stratigraphic insight that is not based on analogy but rather on analysis (Paola, 2000).

Physical modeling, however, is not without its hurdles. Skepticism surrounding experimentation is based on the well-established notion that small-scale modeling of basin-filling dynamics presents formidable scaling problems (Peakall et al., 1996; Paola, 2000). In short, there is no practical way of scaling certain physical aspects of basin filling, such as grain size or fluid viscosity. Thus, if the value of an experiment is assessed by how much it equates with a natural system based on classical formal scaling (e.g., Massey, 1989), i.e., using experiments as analogs, physical modeling leaves much to be desired.

Another way to view experiments is as systems unto themselves and not as scale models or analogs (Hooke, 1968). In this sense, the value of models in geomorphology and stratigraphy becomes their

reliance on similarity of process in establishing the varied interactions between flow and topography, commonly referred to as morphodynamics. In this heuristic approach to modeling depositional systems experimentally, organization arises independently of scale and the details of fluid and sediment properties, creating experimental landscapes that can bear striking similarity to natural systems (e.g., Hasbargen and Paola, 2000; Hoyal and Sheets, in press). For example, braided channel networks exhibit similar geometry over many scales (Sapazhnikov and Foufoula-Georgiou, 1996; Foufoula-Georgiou and Sapazhnikov 2001). This scale independence has supported the use of experimental braided rivers, which evolve quickly, in demonstrating dynamic independence in braided rivers, where channel evolution is statistically similar at different scales (Foufoula-Georgiou and Sapazhnikov, 1998; Foufoula-Georgiou and Sapazhnikov, 2001). More recently Edmonds et al. (2007) illustrated similar spatial organization to experimental and natural distributary channel networks. In erosion-dominated landscapes, such as drainage basins, scale-independent geometry is the norm and has been thoroughly evaluated using fractal geometry (Rodriguez-Iturbe and Rinaldo, 1997). For stratigraphic sciences, similarity in stratal geometry across many scales has been argued (e.g., Vail et al., 1977; Mitchum and Van Wagoner, 1991; Posamentier et al., 1992; Schlager, 2004).

We stress that such similarity does not imply that distortions do not exist at small, experimental scales; at this point, we do not know enough about how such similarity arises to predict how dynamics are modified when scaled down (Paola, 2000; Hickson et al., 2005). With this in mind, we view experiments as tools of analysis, and only by comparing results with models and field observations can we state how completely they capture the dynamics of natural systems.

In the case of the experiment described here, we extract only a small number of controlling variables thought to contribute to sequence-stratigraphic architecture: notably differential subsidence and base-level variation. Of the many parameters not included, wave and tidal processes and climate effects, such as variable water and sediment input, are perhaps most significant. In the context of this discussion, the experiment represents a sequence-stratigraphic base state, where only the most critical boundary conditions are at play, but enough of the relevant dynamics are present to test the relevant sequence-stratigraphic concepts. We justify leaving other parameters out by reasoning that until we understand how stratigraphic surfaces are formed under these relatively simple forcing conditions, adding additional variables simply clouds the insight we are after. Results below demonstrate that even at base-state conditions, the resultant stratigraphy is incredibly complex, containing the primary sequence-stratigraphic disconformities plus additional surfaces that were not expected. Hence, complex stratigraphy can result from relatively simple forcing conditions (Paola et al., 2001). As a final point and one that comes as no surprise, the experiment is not an analog for any natural system. For the time being, it acts as a tangible, quantitative thought experiment; one we believe capable of testing certain sequence-stratigraphic concepts that, in some instances, are outgrowths of qualitative thought experiments on the kinematics of sequence stratigraphy.

EXPERIMENTAL METHODS

Experimental EarthScape Facility

The Experimental EarthScape (XES) facility is located at St. Anthony Falls Laboratory, University of Minnesota, and was created to allow for basin filling under conditions of programmable differential subsidence. The XES facility has been reported on elsewhere (Paola, 2000; Paola et al., 2001; Sheets et al., 2002; Kim et al., 2006; Strong and Paola, 2006, 2008) (Figure 2). Subsidence allows for long-term stratal accumulation and ultimate preservation by slowly removing deposits from the effects of surface reworking. This effect is produced in XES through a specially designed basin floor comprising a honeycomb arrangement of independent subsidence cells (432 in total, 108 used in this experiment; Figure 2). Prior to an experiment, the basin is filled with well-sorted pea gravel that acts

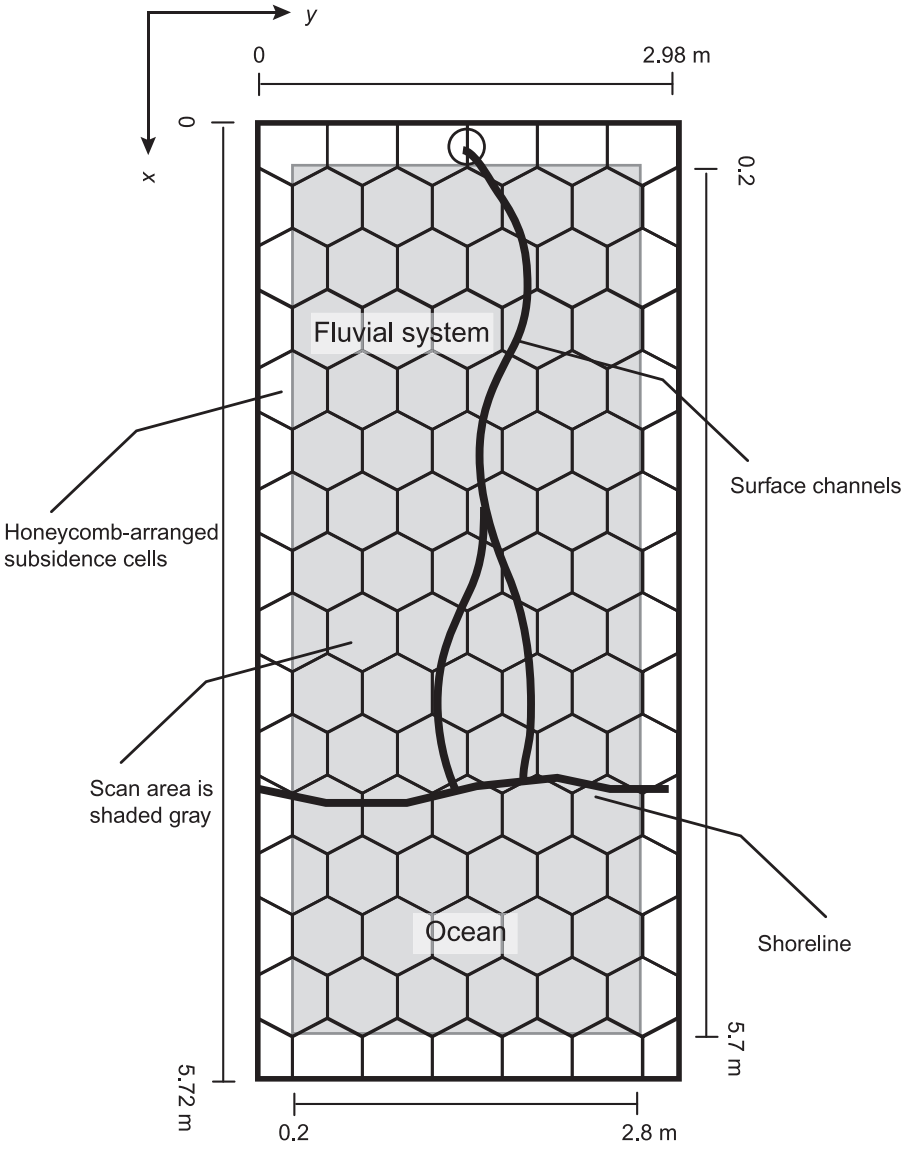

Figure 2. Plan view of the XES basin showing the honeycomb arrangement of subsidence cells. The dimensions of the tank are $0 < x < 5.72$ m (18.76 ft) and $0 < y < 2.98$ m (9.77 ft). Note that the shaded region represents the topographic scan area and has dimensions of $0.2 < x < 5.7$ m (18.7 ft) and $0.2 < y < 2.8$ m (9.1 ft). The schematic fluvial system, complete with channels and shoreline, is physically separated from the subsidence cells by an impermeable rubber membrane (from Kim et al., 2006).

as the basement and is capped by an impermeable rubber membrane. Subsidence is produced by slowly removing the gravel layer through the bases of the subsidence cells (Paola et al., 2001). This procedure, iterated in a precise, choreographed manner, allows for the development of nearly any spatial and temporal subsidence pattern.

Sediment and water inputs are controlled independently of subsidence and can be delivered to the basin at arbitrary locations along the basin boundary. Stratigraphic accumulation occurs on top of the rubber membrane. Base level (the experimental equivalent of sea level) is set by a lake whose elevation is controlled independently of subsidence and (water and sediment) supply via a computer-driven weir.

Experiment Design and Setup

The experiment reported here (henceforth XES 02) was conducted to examine the stratigraphic effects of slow, rapid, and superimposed base-level cycles given a foretilted (downstream-deepening) subsidence profile and constant water and sediment supply (Figure 3). Water supply, sediment supply, and subsidence rate and spatial pattern did not vary during the experiment. The only variable was base level, a choice motivated by the

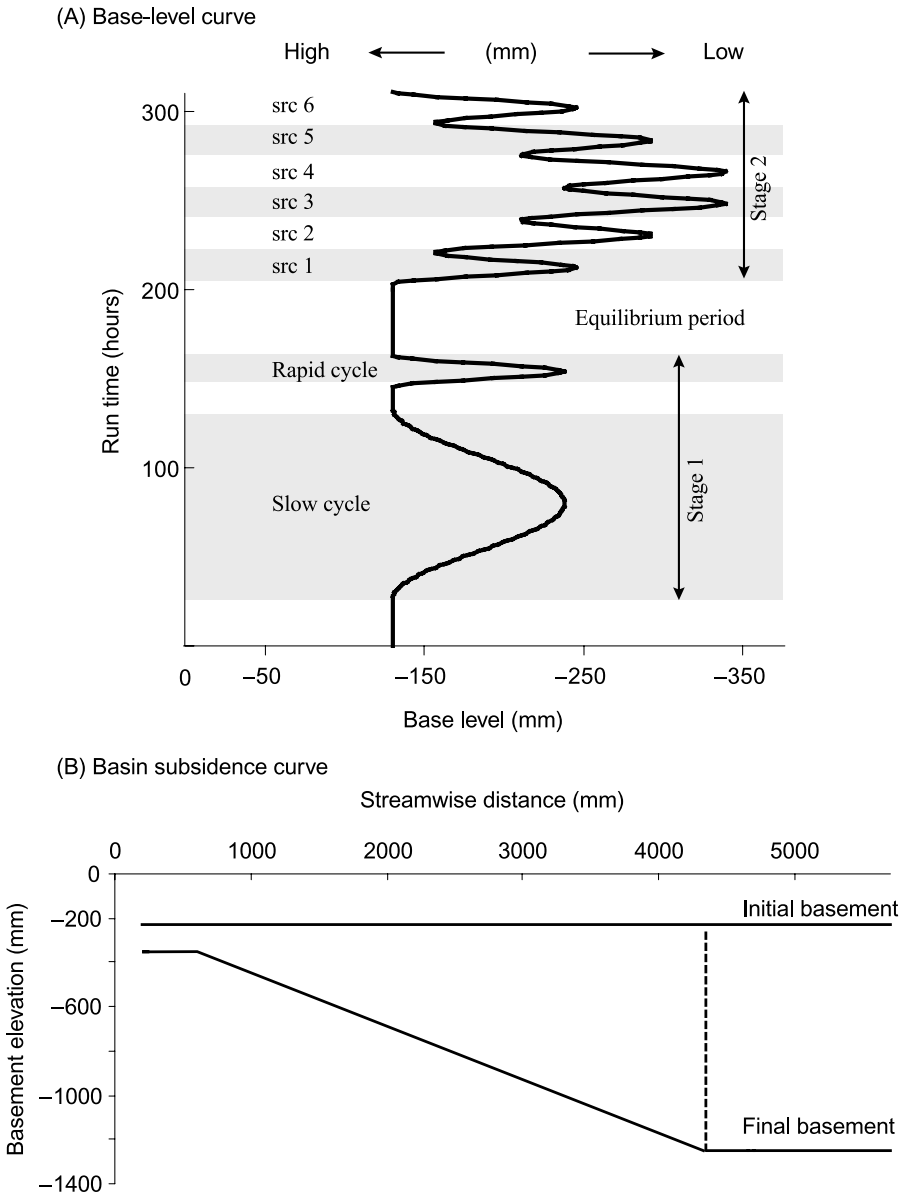

Figure 3. (A) Absolute base-level curve over time for the XES 02 experiment. src = superimposed cycle. (B) Initial and final streamwise basement elevation profiles for the XES 02 experiment; subsidence was constant laterally.

broad class of sequence-stratigraphic models where stratigraphic accumulation is linked to base level (e.g., Frasier, 1974; Vail et al., 1977; Galloway, 1989; Van Wagoner et al., 1990; Posamentier et al., 1992; Plint and Nummedal, 2000). The total duration of the experiment was 310 hr, which was divided into two stages, each examining unique base-level change conditions.

Stage 1 began with 26 hr of constant base level and active subsidence to build an initial deposit. We then imposed one slow base-level cycle, 108 hr long and co-sinusoidal in shape, with 0.11 m (0.36 ft) of base-level drop and rise (roughly five channel scour depths) (Figure 3). This was followed by a 10-hr equilibrium period, then a rapid base-level cycle identical in shape and amplitude to the slow cycle but lasting only 18 hr. The slow and rapid base-level cycles were designed to measure stratigraphic response to base-level forcings with long and short time scales compared to that of the basin equilibrium time (Paola et al., 1992). The geomorphic response is to produce incised valleys during rapid base-level fall and broad erosion with weak valley formation during slow base-level change (Strong and Paola, 2006; 2008).

We followed stage 1 with a 40-hr equilibration period, during which the base level was constant. In stage 2, we superimposed six rapid cycles

on one slow cycle to investigate the stratigraphic effects of two interacting time scales of base-level forcing on the experimental system (Figure 3). The motivation for stage 2 comes from the superposition of sea level cycles with multiple discrete periods caused by, for example, Milankovitch forcing (Crowley and North, 1991). Additionally, detailed seismic and field studies of ancient strata have identified hierarchies of stratigraphic sequences, where smaller-scale sequences are embedded in larger-scale sequences, suggesting past multiharmonic relative sea level fluctuations (e.g., Vail et al., 1977; Goldhammer et al., 1987; Haq et al., 1987; Mitchum and Van Wagoner, 1991; Jones and Milton, 1994).

The plan form area of XES 02 comprised one quarter of the full basin (108 cells; 2.98 × 5.72 m [10 × 20 ft]) (Figure 2). The constant sediment and water supplies were mixed outside the basin and fed through a single pipe located at the center of one of the short sides of the basin. The sediment mixture consisted of 63% 120-μm (very fine) silica sand, 27% bimodal anthracite coal (75% 190 μm and 25% 490 μm), and 10% kaolinite clay. The silica sand acts as the coarse sediment fraction because of its relatively high specific gravity (sg = 2.65), and the coal, though larger, is lighter (sg = 1.3) and behaves as the more mobile sediment fraction. The coal-sand mixture has the added benefit of high optical contrast, making stratigraphic architecture readily apparent. Clay was added to enhance the mechanical strength of exposed vertical faces during deposit sectioning. Compaction effects are negligible because of the relatively small overburden. Subsidence rate $\sigma(x)$ was given by $\sigma(x) = \sigma_0(x/L)$ for $0 < x \leq L$ and $\sigma(x) = \sigma_0$ for $x > L$ where $x = 0$ is the upstream end of the basin, $\sigma_0 = 3.71$ mm/hr, and $L = 4.2$ m (13.7 ft) (Figure 3).

Water discharge, Q_{w0}, and sediment feed, Q_{s0}, were input to the basin at 0.417 and 0.0051 L/s, respectively, resulting in a water-sediment discharge ratio of $Q_{w0}/Q_{s0} = 81.8$. In the context of basin filling, the integrated volume of sediment delivered to the basin over the course of the experiment was a little more than one-half of the total accommodation volume created from subsidence, resulting in an underfilled basin (Paola et al., 1992). This was done to ensure that the delta toe boundary did not contact the distal basin wall.

Data Collection

Over the 310-hr experiment, 101 subaerial and submarine topography scans were collected at intervals ranging from 1.5 to 8 hr, depending on the phase of the experiment. Fluvial topography was recorded by a laser sheet system (0.1-mm [0.003-in.] vertical resolution), and submarine bathymetry by an ultrasonic sonar transducer (1-mm [0.039-in.] vertical resolution). The topographic and bathymetry data for each scan were then merged by a simple interpolation procedure to produce one digital elevation model (DEM) of the entire experimental surface. Because of data problems, we excluded 11 scans, leaving a total of 90 surface DEMs for analysis. The surface of the experiment was photographed with a digital video camera every 2 s and every 30 min with a high-resolution still camera.

After the run finished, we sectioned the deposit to record the stratigraphy. We first serially sectioned half of the deposit in an orientation perpendicular to flow at 0.01-m (0.03-ft) intervals using techniques outlined by Sheets et al. (2002), resulting in 474 stratigraphic faces. The remaining half of the basin was sectioned at 0.01-m (0.03-ft) intervals at an orientation parallel to flow, resulting in 125 stratigraphic faces. We dissected this part of the basin with an automated deposit cutting and imaging system designed and constructed at St. Anthony Falls Laboratory (Mullin and Ellis, 2008). To study the imaged stratigraphy in a 3-D cube, we converted the deposit image files to SEG-Y and created two pseudoseismic surveys of the experimental stratigraphy (one for each half of the basin) (Figure 4). (The pseudoseismic volume constructed from the strike-oriented images is called the strike-oriented volume, and from the other half, we created a dip-oriented data volume.)

To compare the mapped stratigraphic horizons directly with the topographic scans, each surface DEM was migrated for the total amount of subsidence between the scan time and the end

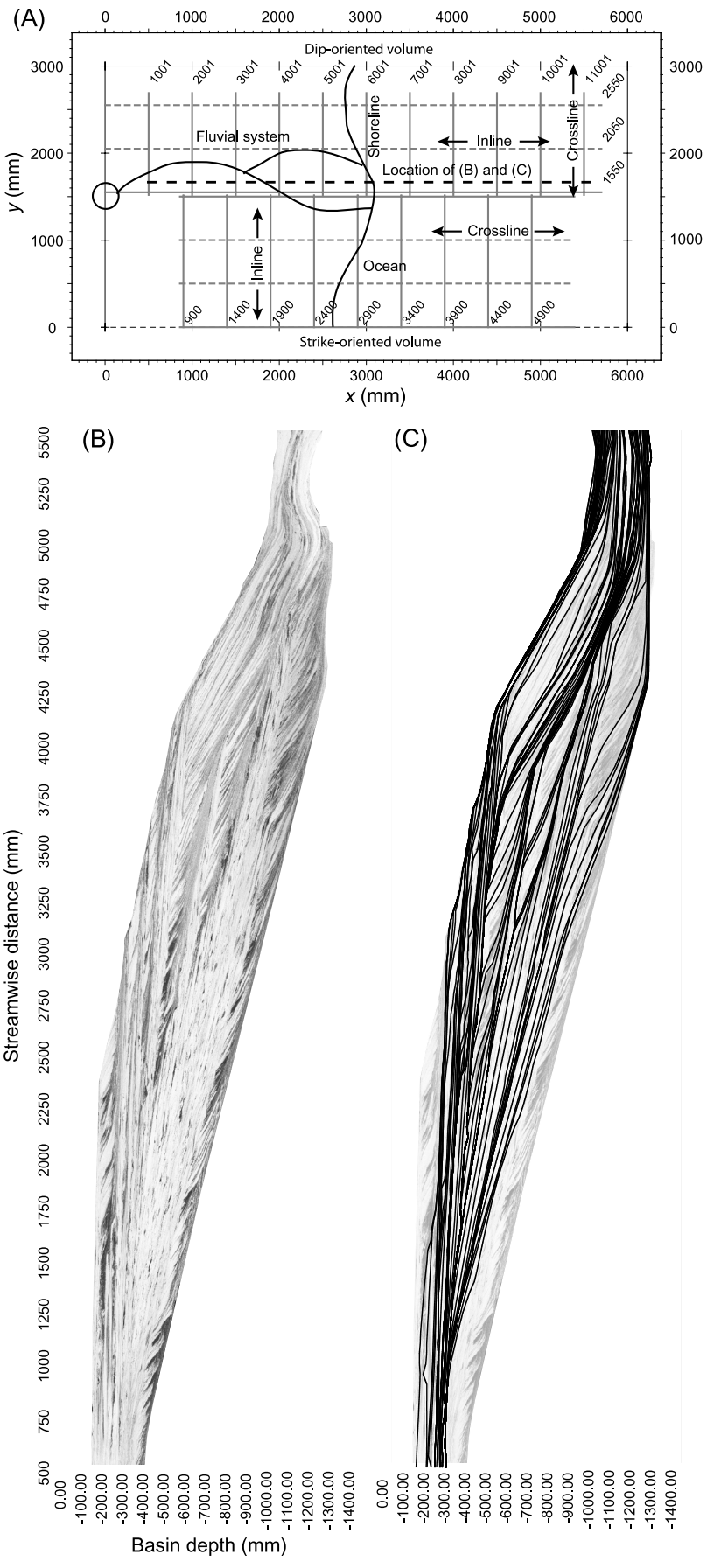

Figure 4. (A) Plan view of the XES basin showing the (top) dip-oriented and (bottom) strike-oriented deposit volumes generated from serially dissecting and imaging the deposit. A schematic of the fluvial system is shown to illustrate the orientation of the sediment-transporting system. (B) Example dip-oriented inline at y = 1550 mm (61 in.). (C) Same example inline with all clipped and migrated topography data overlain, illustrating an intersection of sorts between stratigraphy and time (in the form of preserved topography).

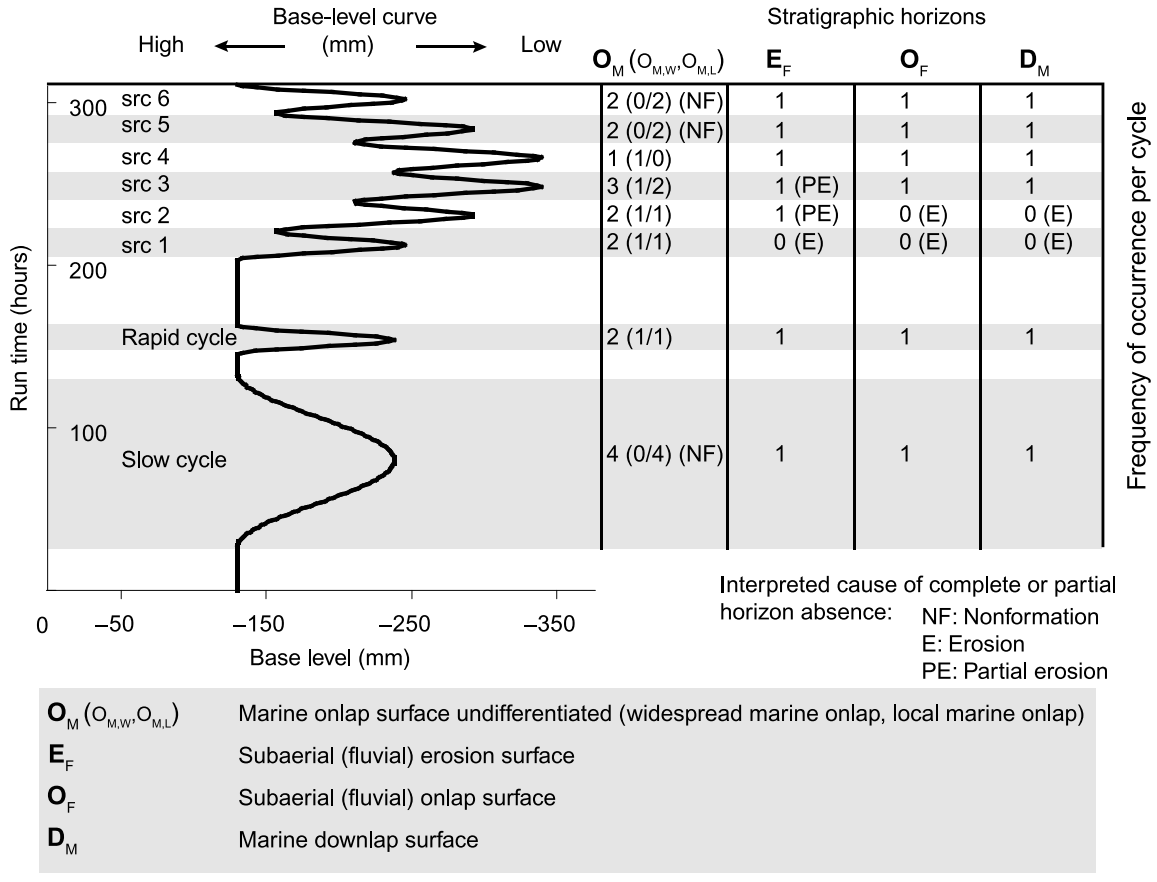

Figure 5. Frequency of occurrence of stratigraphic horizons based on their known associated base-level cycle. Marine onlap surfaces are segregated into allogenic based ($O_{M,W}$) and autogenic based ($O_{M,L}$). Nonformation of O_M refers to the absence of $O_{M,W}$. Erosion and partial erosion refer to the removal of stratigraphic horizons only where they are identified by discordance. For example, D_M is present for superimposed rapid cycles 1 and 2 but cannot be identified by downlap; instead, where they are preserved, the strata are concordant. See the text for further discussion. src = superimposed cycle.

of the experiment, and then clipped to account for erosion after deposition. To clip a surface DEM for erosion, we compared its subsided elevation at all points to each successive scan. At every point where a later elevation was lower than the reference scan, we replaced the original elevation with that of the later scan. The processed DEMs were then loaded into the seismic cubes for comparison with the deposit (Figure 4).

KEY STRATIGRAPHIC BOUNDING SURFACES

We identify and correlate four stratigraphic surfaces based solely on their geometric expression. To emphasize this and avoid confusion with varied sequence-stratigraphic terminology and implications therein, we designate surfaces using symbols: subaerial (fluvial) erosional truncation (E_F), marine downlap (D_M), marine onlap (O_M), and subaerial (fluvial) onlap (O_F) (Mitchum et al., 1977a) (Figure 1). We relate these discordances to the primary stratal terminations outlined in the depositional sequence model (e.g., Mitchum et al., 1977a, and later Van Wagoner et al., 1988, 1990) because it is widely used and, for practical purposes, serves as the reference sequence-stratigraphic model. We note that of the eight imposed base-level and corresponding stratigraphic cycles, some are observed for which the complete suite of horizons listed is not present because of either destruction by subsequent erosion or nonformation; in other cases, more than one horizon exists for the same discordance (Figure 5). Consequently, even in a controlled stratigraphic setting and using the full suite of sequence-stratigraphic concepts, it is

surprisingly difficult to identify all eight imposed base-level cycles in the deposit, underscoring the complexity and incompleteness of depositional transformation. Constraining the time domain and emplacement dynamics of stratigraphic horizons helps in disentangling this complexity.

The D_M Surfaces

The D_m surfaces in XES 02 are nondepositional disconformities with long correlation lengths. They are recognized where marine foresets downlap flat-lying fluvial strata or bottomsets of underlying clinoforms (Figure 6). Downdip, the bounding strata commonly become parallel as clinoform bottomsets overlie fluvial deposits or marine concordant bedding. The updip limit to the D_M surface occurs near its lateral transition to fluvial deposits, where it can no longer be unambiguously identified. No fluvial extension of the D_M is observed. The closest corresponding depositional-sequence stratal contact is the maximum flooding downlap surface (Van Wagoner et al., 1988).

The O_M Surfaces

The O_M surfaces are distinguished by low-angle, or even mounded, foresets that subaqueously onlap onto foresets updip (Figure 6). The longitudinal extent of O_M surfaces is more limited than the other horizons described because of narrow individual foreset profiles and updip truncation by surfaces of subaerial erosion (denoted as E_F and discussed below). The O_M are also generally less persistent across the width of the basin and laterally become conformable. We identify two types of O_M surfaces: relatively widespread O_M, designated as $O_{M,W}$, and local O_M, assigned $O_{M,L}$. Each $O_{M,W}$ is sufficiently widespread that, despite reaches where the strata are conformable, correlation results in one contiguous horizon. In contrast, each $O_{M,L}$ comprises a bundle of local O_M that are laterally separated from each other although they exist at similar streamwise positions. The key distinction of each $O_{M,L}$ is that it does not clearly demarcate a single stratigraphic surface. The sequence-stratigraphic significance of $O_{M,W}$ and $O_{M,L}$ is discussed below, but given their correlation differences, we limit sequence-stratigraphic-significant O_M to $O_{M,W}$.

Applied to the depositional sequence model, $O_{M,W}$ strictly identifies stratal onlap onto the marine part of the sequence boundary (i.e., O_M does not represent coastal onlap) and is named by Embry (2001) as a slope onlap surface.

The E_F Surfaces

The E_F surfaces are extensive subaerial erosional disconformities that are limited to the reach over which fluvial deposits truncate and overlie marine foresets (Figure 6). Updip, where the truncation surface bounds fluvial strata above and below, the definition of E_F becomes difficult as the continuous allogenic surface merges into stochastic fluvial erosion surfaces. Downdip, E_F transitions to a marine conformity (C_M) at the point where we observe preserved clinoform topsets; at this point, the E_F discontinuity terminates. The onset of C_M is marked in marine strata by a basinward transition from persistently truncated clinoforms to foresets packaged as mixed toplapped and complete sets, and in fluvial strata by topset accretion. We point out that although the facies contact between marine and fluvial strata continues basinward of the distal limit of E_F, significant adjustments accompany the above stratal shifts: at the E_F-C_M transition, fluvial thickness generally decreases, and an architectural switch from dominantly channel-fill structures to depositional sheets is observed (cf. Sheets et al., 2002) (Figure 6). In concert with significant topset denudation during relative base-level fall from DEM analysis, the closest geometrically equivalent sequence-stratigraphic horizon is the subaerial part of the depositional sequence boundary (Van Wagoner et al., 1988, 1990; Hunt and Tucker, 1992; Helland-Hanson and Martinson, 1996).

The O_F Surfaces

The O_F surfaces are identified as the lowest stratigraphic position where sedimentation is limited to the clinoform topset (Figure 6). Overlying sediments are packaged into back-stepping units that internally exhibit downlap and onlap onto O_F;

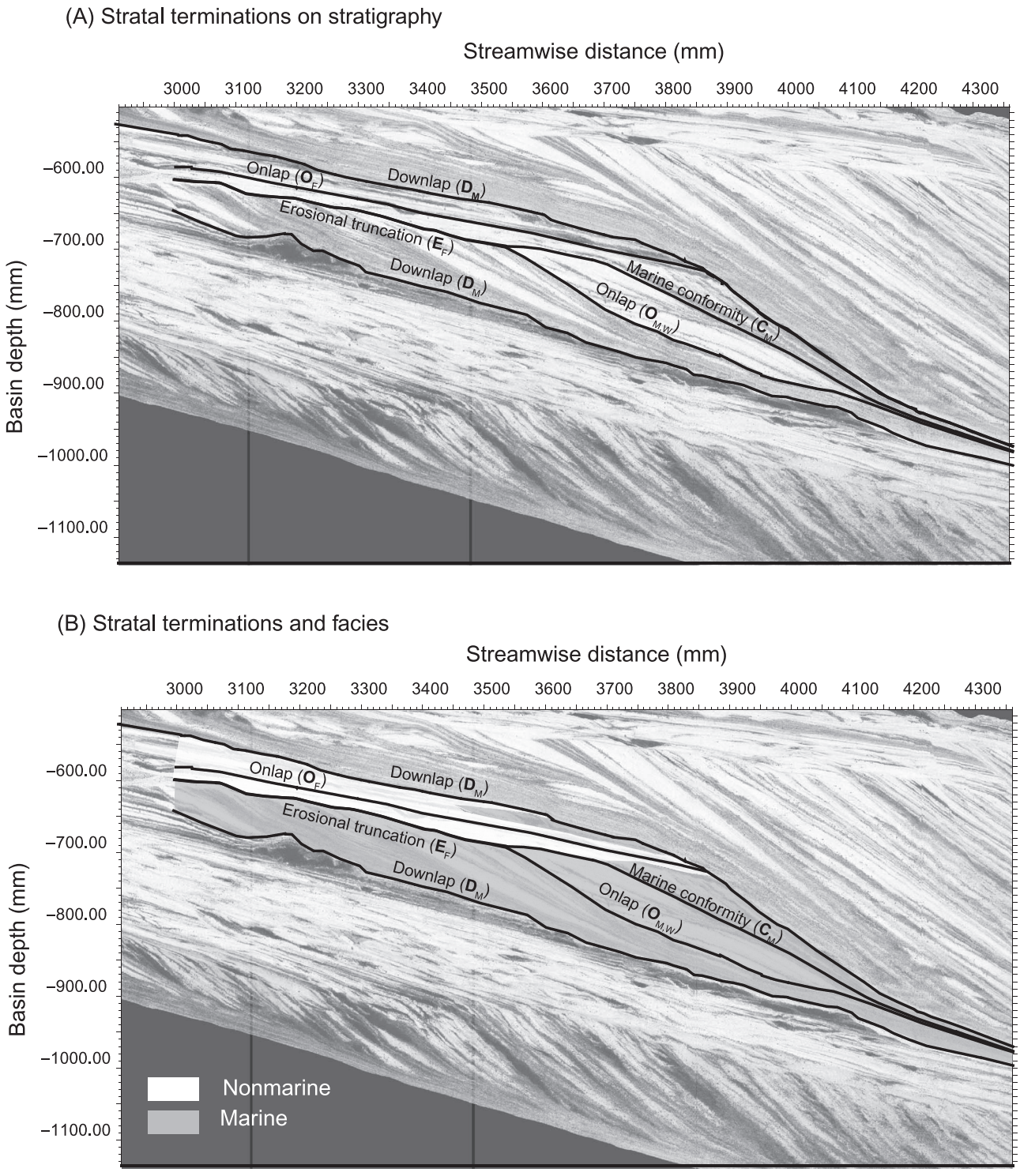

Figure 6. (A) Stratigraphic dip section at y = 2300 mm (90 in.) illustrating the interpreted stratigraphic horizons for the rapid cycle based on stratal contact geometries outlined in Figure 1. (B) Nonmarine and marine facies overlay.

onlap occurs with low angular change. Nested surfaces of autogenic fluvial scour, which are coeval with the progressive burial of O_F, make these surfaces difficult to map and severely limit updip correlation. Downdip O_F merge with D_M. Although onlap onto O_F is not by marine strata (i.e., it does not strictly signify a flooding surface), it demarcates the shift from progradational and aggradational

stacking to retrogradational stacking, which we interpret to be functionally equivalent to the transgressive surface in the depositional sequence (top of lowstand systems tract) (Posamentier and Vail, 1988; Van Wagoner et al., 1988, 1990). Importantly, O_F surfaces are not erosional unconformities (in the experiment, E_F are the only subaerial erosional surfaces) nor do O_F signify onlap onto E_F, which are always buried by the time of O_F formation.

TIME SIGNIFICANCE OF STRATIGRAPHIC SURFACES

For a stratigraphic surface to have time-stratigraphic significance, it must separate younger, overlying strata from adjacent older, underlying strata over its correlated area. More precisely, a preserved stratigraphic surface has chronostratigraphic significance to the extent that it coincides with the geomorphic surface for an instant or an interval of time. Stratigraphic surfaces that form diachronously can also be chronostratigraphic markers to the extent that there is at least one time for which all of the points that comprise the stratigraphic surface formed the geomorphic surface. We point out that our definition is different and more restrictive than Mitchum et al. (1977a), who, by virtue of regional two-dimensional seismic data, applied chronostratigraphic significance in an expanded sense, focusing instead on stratigraphic hiatuses over much broader time scales (e.g., geochronologic units) and inferring similarly broad depositional trends. Although different, these metrics of time stratigraphy certainly complement each other, where in the experimental case time stratigraphy can be evaluated mechanistically through comparisons between stratal horizons and paleotopography. Here we evaluate the linked geomorphic and chronostratigraphic implications of stratal surfaces defined by marine downlap and onlap (D_M, O_M), subaerial erosional truncation (E_F), marine conformity (C_M), and subaerial onlap (O_F).

The D_M Surface Equivalence

Direct comparison with measured topography reveals that, over the correlated streamwise reach of D_M, they closely match most topographic scans collected during periods of base-level rise because of offshore sediment starvation (Figure 7). Consequently, on average, D_M correspond to positions of base level around the inflection point of the rising limb of the base-level curves despite variability in deposit surface geometry and base-level rise curves. These results broadly accord with sequence-stratigraphic models, which show D_M to be a robust record of relative rise of sea level (Posamentier et al., 1988; Van Wagoner et al., 1988, 1990; Galloway, 1989; Hunt and Tucker, 1992; Embry, 1993).

In the case of the maximum flooding surface, the critical instant when the stratigraphic surface most widely matches the geomorphic surface occurs at the time when the shoreline is at its most marginward position (Posamentier et al., 1988; Galloway, 1989; Catuneanu, 2002). In the experiment, the strongly in-phase relationship between base level and shoreline position results in maximum transgression at base-level highstand and not at the inflection point of the rising limb, which leads to a persistent temporal and spatial gap between D_M and topography associated with the most landward shoreline position (Figure 7). The general displacement between D_M and topography in the experiment is caused by offshore sedimentation during the remaining period of the base-level rise. Although minor, it repeatedly elevates the topography scan at base-level highstand above D_M. Consequently, even during periods of relative depositional quiescence, precisely matching stratigraphic surfaces to their theoretical surface equivalents is difficult.

The O_M Surface Equivalence

The $O_{M,W}$ surfaces strongly correlate to time lines near the inflection point of base-level fall and typically (though not always) when the rate of base-level fall is increasing. Furthermore, several preceding scans also conform to $O_{M,W}$, suggesting that prior to onlapping marine deposition these surfaces represent condensed intervals or bypass (Mitchum et al., 1977a). The $O_{M,W}$ have additional value because their preservation potential

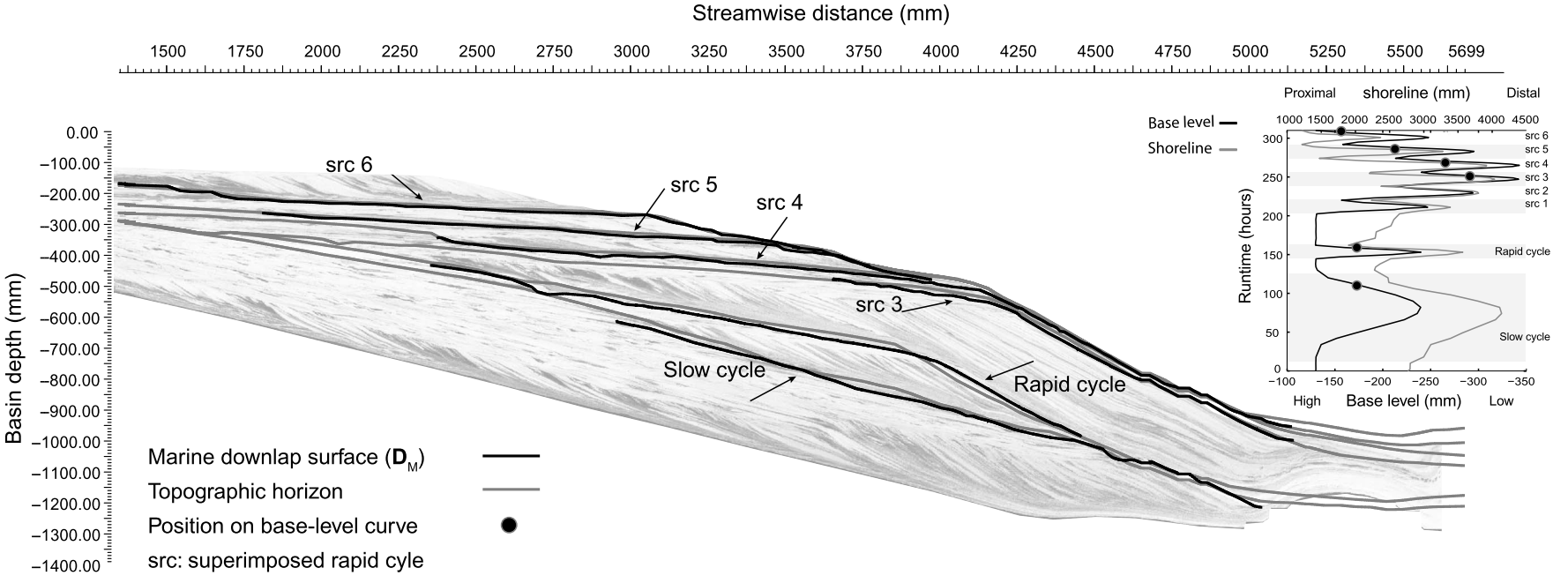

Figure 7. Dip-oriented stratigraphic panel at y = 1550 mm (61 in.) illustrating the association between all mapped D_M and nearest topographic scans. Times of topographic data collection are plotted on the base level and shoreline curves. src = superimposed cycle.

is greater than any other stratigraphic surface formed in XES 02. (This is because O_M discordances occur at relatively low elevations in the depositional profile.) This fact is highlighted for superimposed cycles (src) 1 through 3. This set comprises rapid cycles superimposed on slowly falling base level. They leave no clear stratigraphic signature in the updip part of the basin: Each incised valley tends to cut out the preceding one. Using conventional indicators (e.g., erosional unconformities), the package could appear to consist of only one sequence (Figure 8). Looking offshore, however, $O_{M,W}$ unequivocally break out these three stratigraphic packages amidst a thick succession of otherwise enigmatic foresets (Figure 8).

The O_M can be difficult to interpret, however, because local O_M and $O_{M,L}$ coexist with $O_{M,W}$: In XES 02, all stratigraphic cycles except src 4 contain multiple O_M, which if not differentiated could lead to an overinterpretation of the basin fill history (e.g., a more complicated relative sea level curve) (Figure 5). In addition to correlation differences between $O_{M,W}$ and $O_{M,L}$, we discuss below how O_M may potentially be differentiated into its allogenic-sourced ($O_{M,W}$) and autogenic-sourced ($O_{M,L}$) forms by incorporating the stratigraphic length over which the discordance persists.

The E_F Surface Equivalence

Comparative analysis reveals that E_F crosscut topographic time lines, which document diachronous E_F formation (Figure 9). Kinematically, E_F development corresponds to rapid, forced-regressive shoreline migration associated with significant fluvial erosion and bypass to accreting marine foresets (e.g., Hunt and Tucker, 1992; Posamentier et al., 1992). All E_F, however, are consistently lower than surface scans collected during fluvial downcutting. The vertical offset is significant, up to three channel depths. The result is E_F surfaces that do not closely coincide with any instantaneous geomorphic surface that ever existed (Strong and Paola, 2006, 2008) (Figure 9). That is, no demonstrable synchroneity to E_F exists.

The E_F Chronostratigraphic Significance

The large difference between E_F and associated topographic profiles is noteworthy because it does not support a clear chronostratigraphic connotation for the E_F. We explore this point further with topographic data analysis, where we can quantitatively evaluate the geomorphic approximation and therefore the chronostratigraphic meaning of the topographic-based E_F. We create a synthetic erosional surface, denoted as E_F^T, point by point by finding the lowest topographic elevation among all DEMs measured during a rapid base-level cycle. (The E_F^T surface is an imperfect approximation to E_F because of the limited time resolution of the measured topography.) For each position, we then find the time at which the E_F^T was emplaced (Strong and Paola, 2006, 2008). To measure fluvial retention during base-level fall, where E_F^T was emplaced prior to base-level lowstand, we measure the preserved depositional thickness over the remaining base-level fall time.

Results for superimposed rapid cycle 2 are shown in Figure 10 where we observe two important features. First, the E_F^T surface is created during base-level fall and part of the rise, consistent with the findings of Strong and Paola (2006, 2008) (Figure 10A), resulting in strong nonequivalency between E_F^T and any instantaneous topography (including the surface geomorphology at the base-level minimum) (Figure 10B). Second, the time-transgressive evolution allows for the possibility of E_F^T formation and burial by preserved fluvial deposits during base-level fall, which we show to be the case here (Figure 10C). This result is a physical demonstration that some strata overlying the erosional unconformity are contemporaneous with or even older than underlying, basinward strata. We stress the point that fluvial trapping occurs in an experimental system that is in some ways optimized for fluvial bypass because of a short fluvial reach and a relatively high water discharge. Thus, fluvial deposition during base-level fall is likely to be more common in the field than currently recognized, as proposed by Blum and Tornqvist (2000) and Blum and Aslan (2006) based on field observations. The amount of preserved

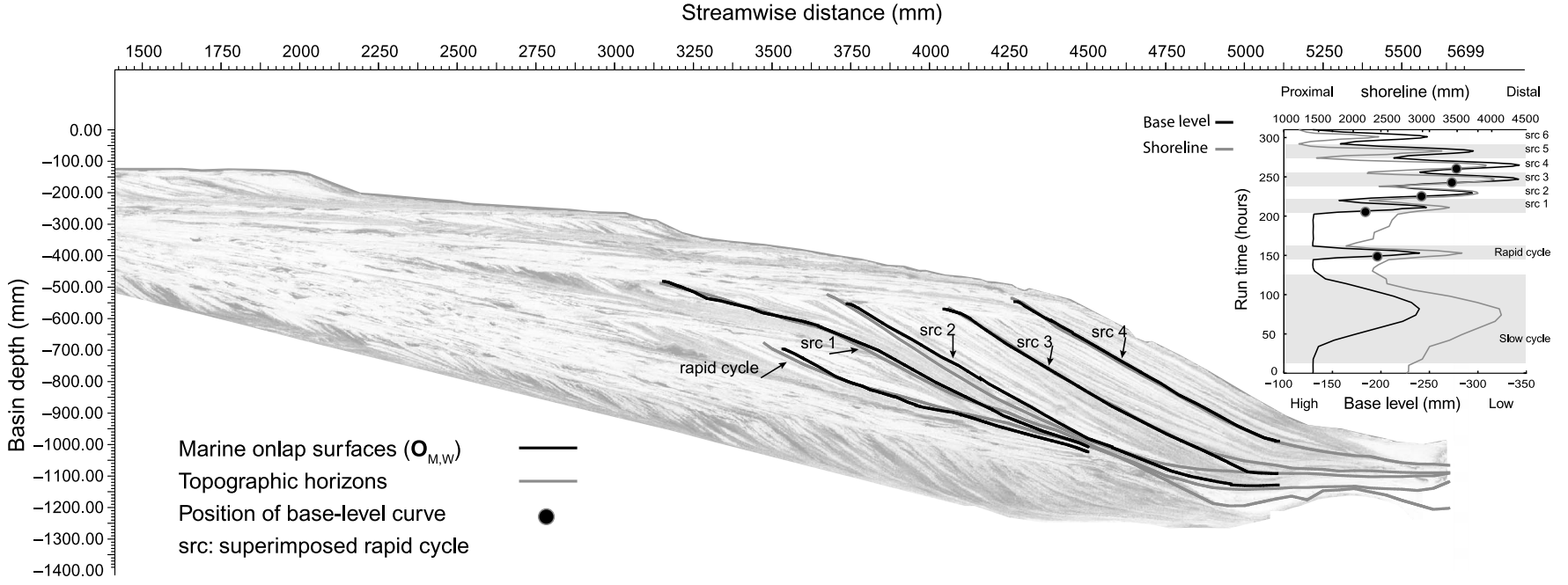

Figure 8. (A) Dip-oriented stratigraphic panel at $y = 2300$ mm (90 in.) illustrating the association between all $O_{M,W}$ and the nearest topography. Times of topographic data collection are plotted on the base level and shoreline curves. src = superimposed cycle.

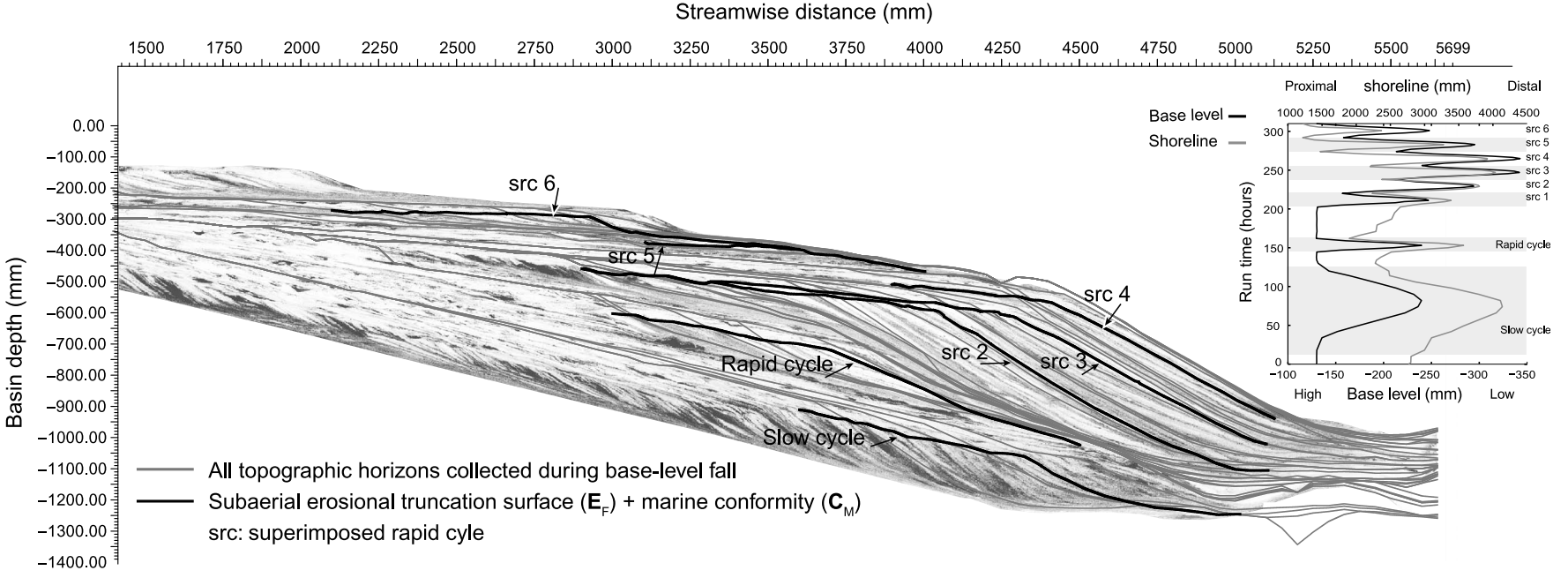

Figure 9. Dip-oriented stratigraphic panel at $y = 2300$ mm (90 in.) illustrating the relationship between all interpreted $E_F + C_M$ and topographic data collected during all periods of base-level fall. Note that the presence of the E_F associated with src 3 is above the E_F associated with cycle 2, although the base-level minimum of cycle 3 is lower than 2. The partial preservation of cycle 2 E_F is caused by subsidence.

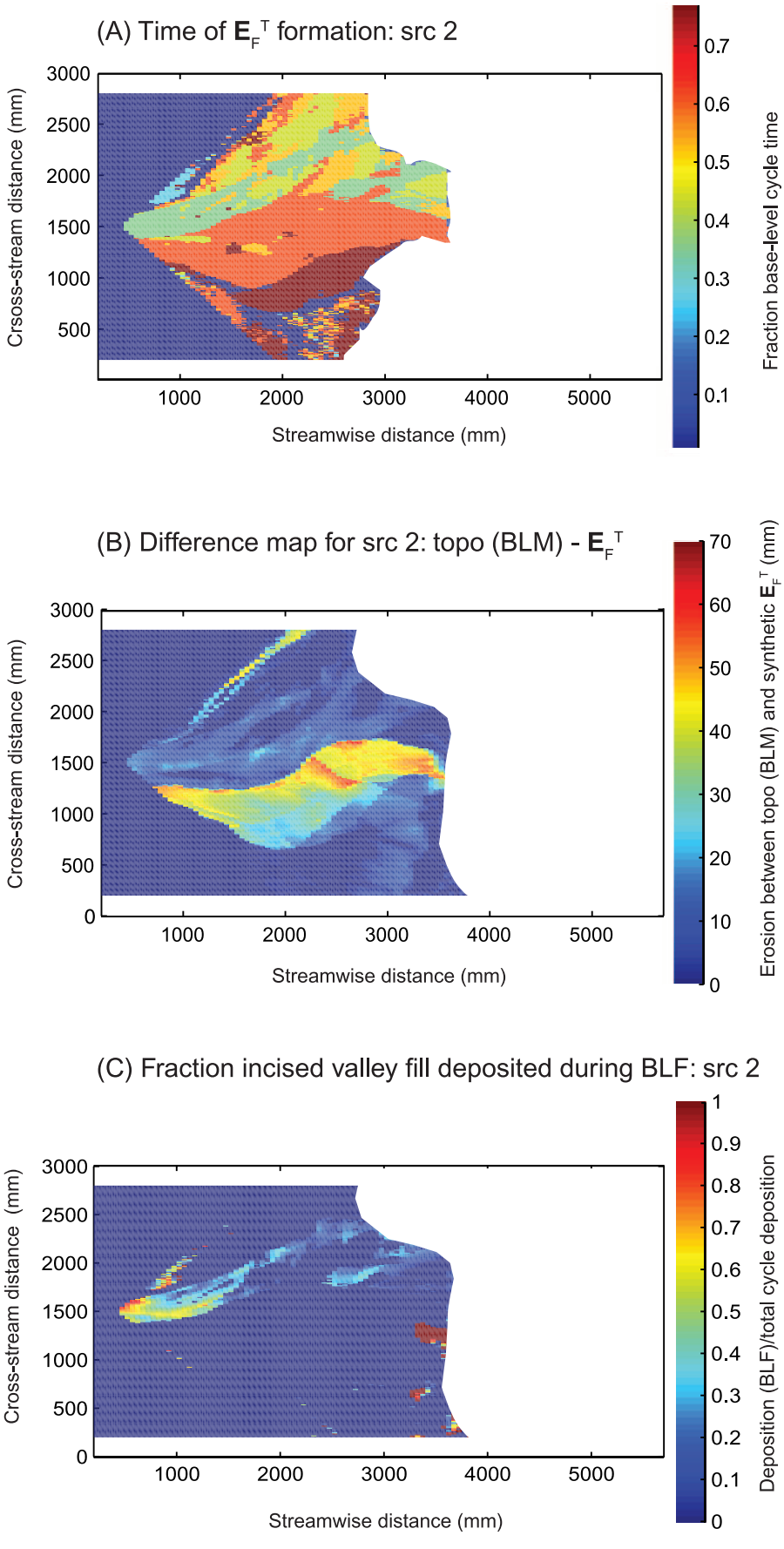

Figure 10. (A) Map showing the formation time of the synthetic E_F, E_F^T, for superimposed base-level cycle 2. (B) Map illustrating elevation differences between the instantaneous topography at base-level minimum (BLM) and E_F^T, and thus the nonequivalence between the two. (C) Distribution of fluvial deposition during this period of base-level fall (BLF), documented as a fraction of the total incised-valley-fill thickness. Preserved falling-stage deposition removes E_F^T from having absolute chronostratigraphic significance. src = superimposed cycle.

valley deposition during base-level fall captured in the DEM analysis is influenced by the DEM collection frequency (increasing the scan recurrence interval results in a smaller chance of capturing falling-stage fluvial deposition). Consequently, the preserved valley deposition during the falling base level accounted for in this example should be considered a minimum estimate.

The C_M Surface Equivalence

The C_M surface by definition is conformable, and along any one dip horizon, the C_M approximates a time horizon. Laterally, however, C_M corresponds to unrelated foreset surfaces. This prohibits a definitive lateral correlation and removes C_M from any obvious geomorphic equivalence as one throughgoing surface (Catuneanu et al., 1998). Paleotopography shows that various C_M do bundle very near base-level minimum, however, and in the experiment can be used as recorders of approximately base-level minimum.

The O_F Surface Equivalence

The O_F surface is the stratigraphic record of the onset of back-stepping deposition during base-level rise. Matching to topography data is difficult because it does not reflect stratigraphic condensation (as is the case for D_M and $O_{M,W}$). However, we argue that because the O_F is an active fluvial surface, it cannot have strong time significance, primarily because of the autogenic fluvial modification of the O_F as it is progressively buried (Muto and Steel, 2001; Kim and Muto, 2007). However, over its correlated area and where measurable, the time span of O_F formation is relatively short when compared to E_F.

EMPLACEMENT MECHANICS OF STRATIGRAPHIC SURFACES AND RELATION TO THE FIELD

Broad similarity in horizon juxtaposition and deposit geometry between XES 02 stratigraphy and the field (i.e., natural sequence-stratigraphic successions) (e.g., Mitchum et al., 1977b; Van Wagoner et al., 1990) indicates that the sediment mass-balance control on horizon development is mostly scale independent (Posamentier et al., 1992). This is because the construction of these stratigraphic surfaces in general appears to be controlled by shifting mass balance under changes in accommodation and by generic responses to these shifts (e.g., valley formation) that are independent of scale-sensitive transport details. This point is tested in detail below, but is supported by the fact that geometric models can generate realistic model sequence stratigraphy and provide insight without coupling surface geometry to transport laws (e.g., Jervey, 1988; Lawrence, 1994; Cross and Lessenger, 1998; Perlmutter et al., 1998). Below we qualitatively describe formation processes for the O_M and E_F surfaces, two stratigraphic surfaces that could benefit most from improved process understanding.

The O_M Sedimentary Processes

Off-axis accretion and downstream spreading of individual clinoform lobes laterally produce onlap discordances in cross section, independent of the details of base-level change, and in principle can occur as long as marine deposition is active. The result is multiple O_M in most of the stratigraphic cycles. In XES 02, the key distinction between $O_{M,W}$ and $O_{M,L}$ is the amount of sediment involved in their production: generally, $O_{M,W}$ generation involves significant fluvial erosion and bypass, strongly enhancing sediment flux across the shoreline and deep-marine sedimentation; in contrast, mapped $O_{M,L}$ occur when base-level fall is relatively slow and/or decelerating. Experimental measurement quantifies this point by revealing that, for the isolated and superimposed rapid cycles 1 through 4, the shoreline sediment flux associated with $O_{M,W}$ was up to three times the flux linked to the times of $O_{M,L}$ formation. Note then that despite a much richer variety of gravity-flow mechanisms in the field, the experimental results demonstrate similar mass-balance effects that drive $O_{M,W}$ formation in sequence stratigraphy: voluminous sediment bypass to accreting submarine fans (Mitchum, 1985; Posamentier et al.,

1988). In addition, fluvial incision during accelerating base-level fall restricts lateral channel-belt mobility. Focused sediment flux to marine foresets increases marine lobe amplitude (i.e., foreset variability) via stronger localized progradation. This increases the potential for lateral clinoform accretion by enhancing lateral submarine topography, an effect observed for O_M formed during the isolated rapid cycle and src 1 (Figure 11).

The expected stratigraphic result from increased shoreline sediment flux and focusing is greater lateral persistence of $O_{M,W}$ relative to $O_{M,L}$; this is expressed in the XES 02 stratigraphy as singular $O_{M,W}$ horizons versus bundles of laterally separated but longitudinally collocated $O_{M,L}$. The use of O_M lateral persistence in interpretation is illustrated Figure 12, where the occurrence of all measured O_M is plotted as a function of cross-stream position, and where it is an easy exercise to visually distinguish $O_{M,W}$ from $O_{M,L}$. To quantify this plot and discuss length scales meaningfully, we express the lateral length of O_M as β, normalized by a characteristic channel width b_{ch} to produce a dimensionless length β^*, where $\beta^* = \beta/b_{ch}$ and b_{ch} is approximately 120 mm (4.7 in.) (Sheets, 2004). The probability-density distribution of β^* is also shown in Figure 12, which shows that β^* is mostly ≤1, i.e., most of individual discordances mapped are less than one channel width. We characterize significant O_M lateral accretion to be the tail in the distribution $\rho(\beta^*)$, specifically $\beta^* \geq \beta'$, where β' is a characteristic β^* that defines the 95th percentile of O_M lengths and is solved for by fitting an exponential function $f(\beta^*)$ to $\rho(\beta^*)$. This leads to $\beta' = 1.75$ using the experimental data. We find that all O_M for which $\beta^* \geq \beta'$ correspond to O_M segments that partially form $O_{M,W}$. That is, sequence-stratigraphic-significant O_M, the ones that form $O_{M,W}$ horizons, are persistent over lengths greater than or equal to approximately two channel widths. The specific values probably do not generalize, but the method could be used to distinguish intrinsic from externally forced marine onlap surfaces.

Given the criterion above, $O_{M,W}$ may not form if the offshore sediment flux is too small. More generally, if the allogenic forcing is not capable of amplifying O_M generation beyond the limits of $O_{M,L}$, then no clear sequence-stratigraphic-significant onlap will emerge. This is the case for the experimental slow cycle and superimposed rapid cycles 5 and 6, where in each instance the lowest O_M is $O_{M,L}$ but correspond in bulk to base-level positions at about the inflection point of base-level fall, similar to all of the mapped $O_{M,W}$.

The E_F Sedimentary Processes

The E_F surfaces result from the cumulative effect of the deepest scours during periods of alluvial downcutting (Figure 9). This surface is not coincident with any surface topography and suggests that valley deposition is an important factor during base-level fall because it significantly elevates the minimum surface topography above the E_F and was shown to lead to preserved fluvial deposition in the topographic data analysis above (Figure 10). Fluvial deposition during base-level fall has been shown for several well-constrained Quaternary incised-valley-fill sequences (Blum et al., 1995; Blum and Tornqvist, 2000; Blum et al., 2000). The common, scale-independent element is that bypass becomes increasingly difficult to maintain downstream as more sediment is entrained from the updip valley. The bypass condition implies that streamwise increases in sediment supply from erosion increase transport slope, resulting in a convex-up fluvial profile. Blum and Tornqvist (2000) pointed out that, for many Quaternary valley systems, this transport condition would have been difficult to satisfy, primarily because a convex-up profile would have required more shelf incision than could be provided by base-level lowering during the last eustatic sea level fall. The result is that sediment eroded upstream is sequestered on its way to the shoreline, and some of these deposits may remain at the end of base-level fall.

Another dynamic exemplified in XES 02 is that channel scour is the physical agent that forms E_F, but it is an autogenic process that exhibits a random component on all but very short time scales. Consequently, the actual formation of E_F is spatially and temporally stochastic. One important consequence of this is that the hiatuses associated with the E_F surfaces outlined here are

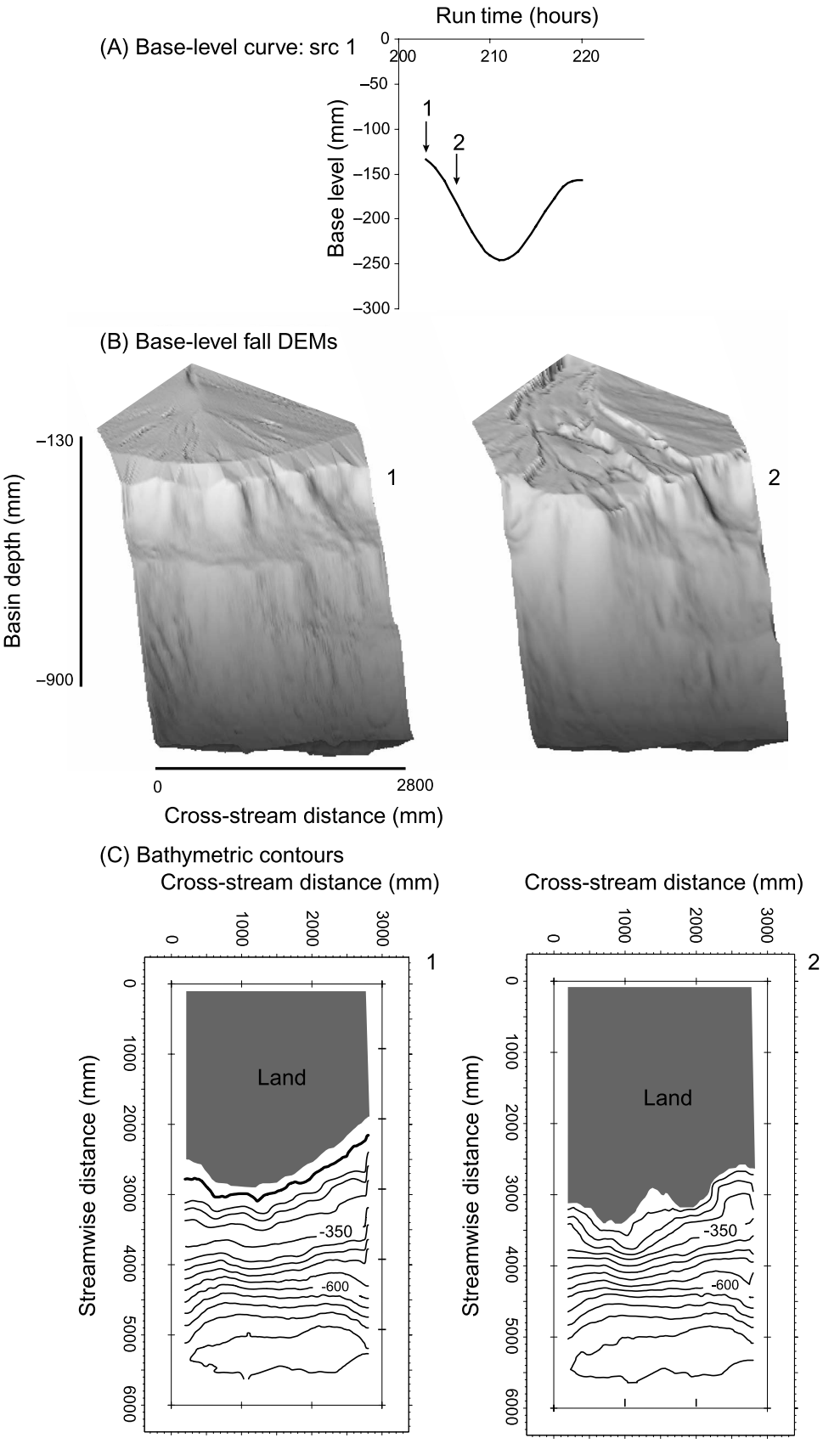

Figure 11. (A) Base-level curve for superimposed rapid cycle 1. (B) Two surface digital elevation models (DEMs) during base-level fall illustrate an increase in bathymetric roughness and therefore potential for laterally accreting clinoforms. (C) Associated bathymetric contour maps quantify this point. src = superimposed cycle.

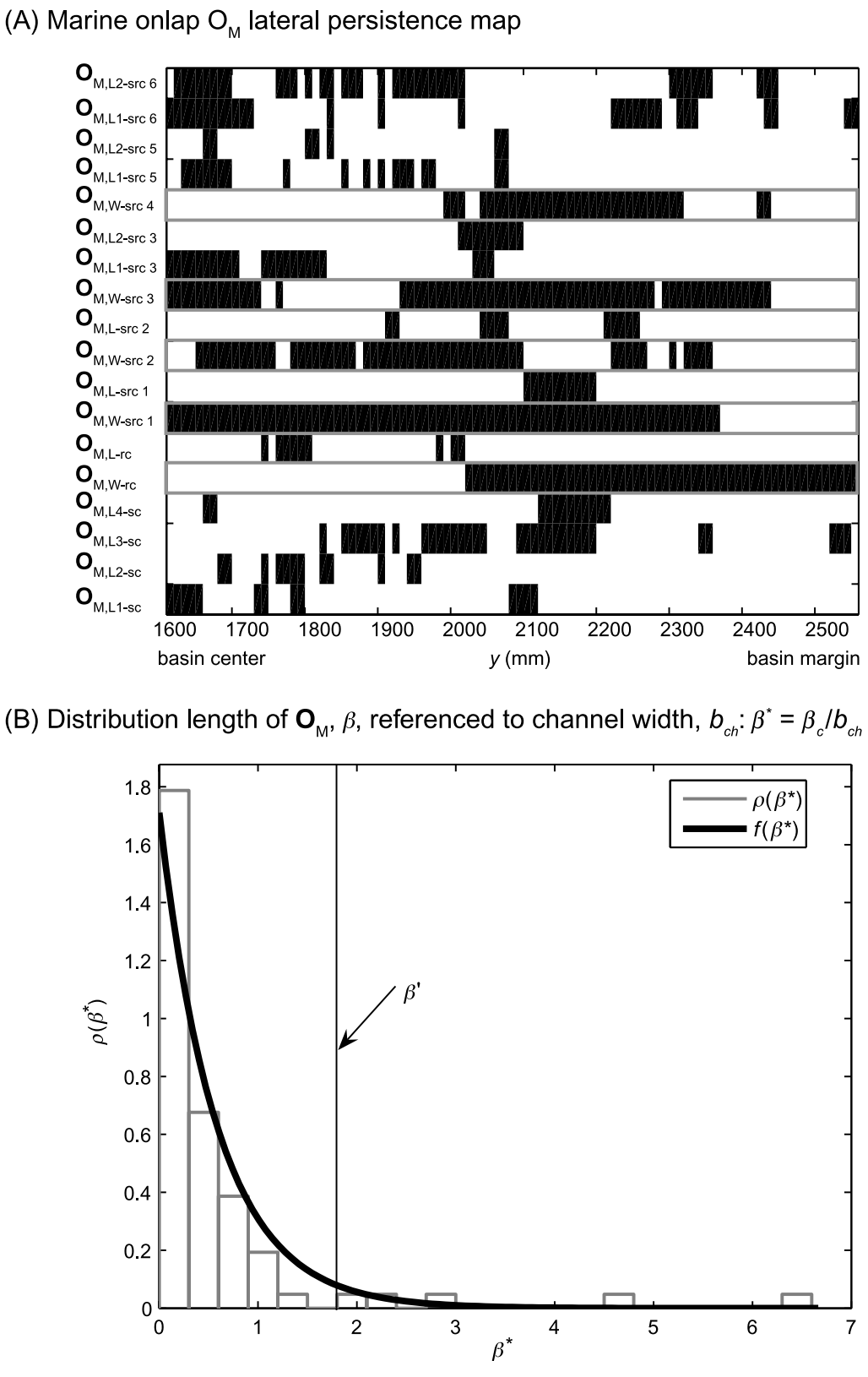

Figure 12. (A). Map of marine onlap (O_M) occurrence for all O_M surfaces. Horizons are labeled on the left, where in the case of multiple $O_{M,L}$, they are labeled $O_{M,L1}$, $O_{M,L2}$, etc.; in addition, the name of the associated base-level cycle is listed (e.g., the second mapped $O_{M,L}$ in superimposed cycle [src] 3 is labeled $O_{M,L2\text{-}src3}$). The $O_{M,W}$ and $O_{M,L}$ are distinguished by our ability to connect them with one horizon. (B) Density distribution of the lateral persistence of individual O_M. The distribution of O_M lengths in XES 02 is exponential and we apply a threshold length β', where β' corresponds to the 95th percentile of O_M lengths and physically represents a length scale of about two channel widths. The O_M lengths $\geq \beta'$ correspond to O_M segments that fall along $O_{M,W}$ horizons, illustrating that these horizons consist of segments greater than or equal to two channel widths. sc = slow cycle; rc = rapid cycle; src = superimposed cycle.

variable, especially considering that individual scour and fill features form and dissipate quickly compared to topographic scan frequency during base-level fall. A similar ambiguity of widespread erosional surfaces has been documented in the field by Tornqvist et al. (2003), who find that

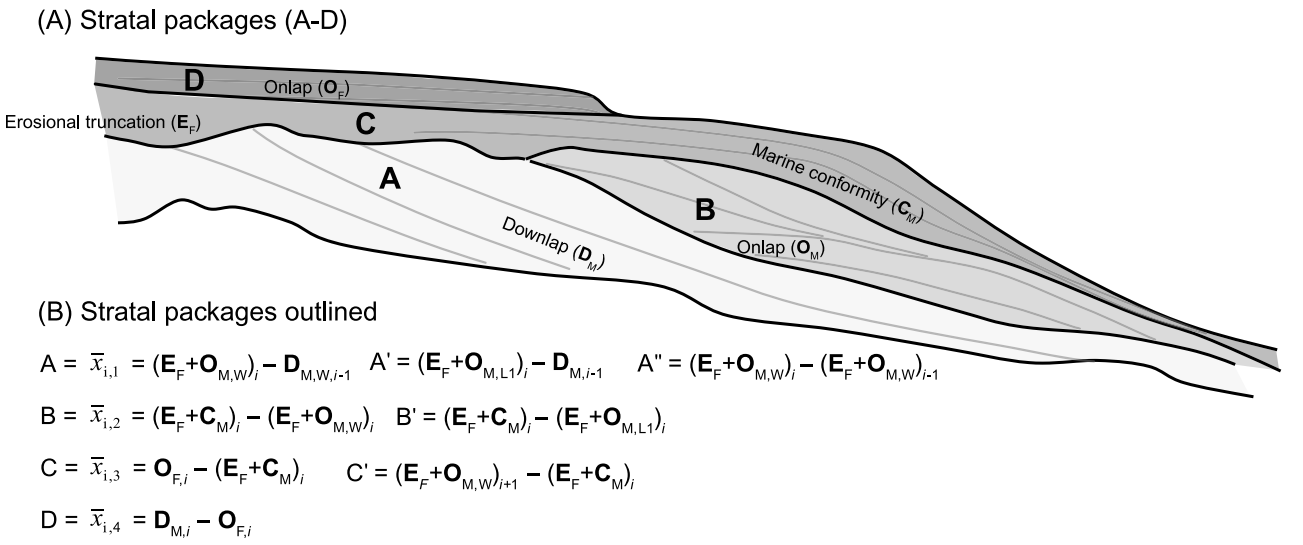

Figure 13. (A) Graphical representation of bounded stratal successions used to calculated sediment mass migration. (B) Full suite of bounded stratal types used in mapping stratal bodies because in some cases the full suite of preserved surfaces shown in panel A are not present. Note that, in a few instances, we use $O_{M,L}$ where no $O_{M,W}$ exists (e.g., for the slow cycle and src 5–6). This was done to maximize the precision of the stratigraphic centroid because in these cases we can constrain the time of $O_{M,L}$ formation. (C) Continuous (green line) and discrete (points) migration of the preserved depositional centroid through time. Error bars on the stratigraphic centroid positions refer to the approximate time span of accumulation. src = superimposed cycle.

the time gap represented in the sequence boundary associated with the last Quaternary eustatic sea level fall (~10 ka) is much shorter than the time span of the fall itself (~ 100 ka).

QUANTIFYING AND TRACKING SEDIMENT MASS MIGRATION

The interpreted stratigraphic horizons in XES 02 result from, and are primary indicators of, shifts in the basinal mass balance. In this regard, stratigraphic surfaces have been used in sequence stratigraphy to construct chronostratigraphic diagrams of preserved deposition, although mainly to highlight their interpreted time significance and coastal onlap. Our emphasis here is to measure how the bounded strata compare to the known mass-balance history of the basin fill, providing a first test of the core product of chronostratigraphic charts (Wheeler, 1958; Vail et al., 1977). Here we propose a quantitative method for measuring the center of depositional mass between stratigraphic horizons, with the goal of comparing discretized stratigraphic migration with the continuously known depositional history.

The Centroid

What is the best reference point for a depositional body? Historically, this location, commonly referred to as the depocenter, has been defined as the location of thickest deposition. Although certainly an important descriptor of sedimentation, this measure does not account for the distribution of deposition. We prefer to define the depositional center as the mean depositional position, which is located by incorporating the spatial distribution of sediment. Formally, the depositional center of mass, termed the centroid, is mathematically defined as the position where a solid body of arbitrary shape is in gravitational balance and is calculated as

$$\bar{x} = \frac{1}{v}\int_R x\delta(x,y)\mathrm{d}A \qquad (1)$$

$$\bar{y} = \frac{1}{v}\int_R y\delta(x,y)\mathrm{d}A \qquad (2)$$

where the centroid position is given by $(\bar{x}, \bar{y})$, $\delta(x, y)$ is the preserved thickness at an arbitrary location in the domain R of the bounded strata, and v is the total volume of the bounded strata. In a

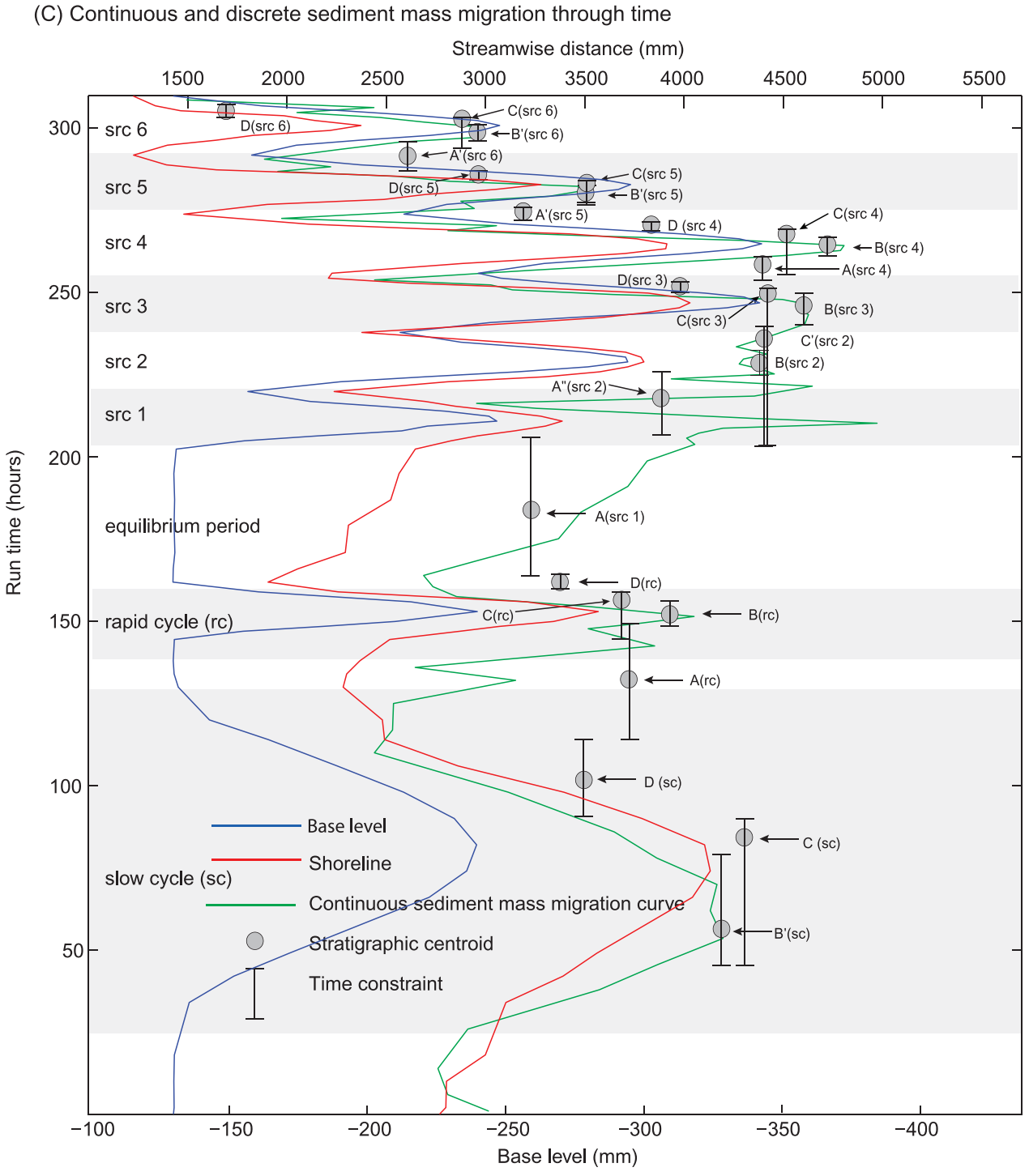

Figure 13. Continued.

time-space diagram commonly applied to stratigraphic sequences, the streamwise centroid $\bar{x}(t)$ is simply the weighted average depositional position for a given time interval; it is a complementary measurement to the presence-absence nature of time-space charts because it considers the shape and magnitude of deposition.

In the case of the topographic-based centroid, $\bar{x}(t)$ is derived from thickness data between consecutive clipped and migrated topographic scans.

This affords a continuous plot of preserved depositional position through time, thereby serving as the solution and reference for comparison with the actual stratigraphy (Figure 13). For the stratigraphic-based centroid, we derive $\bar{x}(t)$ from neighboring stratigraphic horizons whose time range is constrained by topographic time lines. For example, in the *i*th stratigraphic cycle, we map the positions of up to four stratal packages, depending on horizon presence:

$$\bar{x}_{i,1} = f\left[(\mathrm{E_F} + \mathrm{O_M})_i - \mathrm{D_{M}}i-1\right] \quad (3)$$

$$\bar{x}_{i,2} = f\left[(\mathrm{E_F} + \mathrm{C_M})_i - (\mathrm{E_F} + \mathrm{O_M})_i\right] \quad (4)$$

$$\bar{x}_{i,3} = f\left[\mathrm{O_F}i - (\mathrm{E_F} + \mathrm{C_M})_i\right] \quad (5)$$

$$\bar{x}_{i,4} = f[\mathrm{D_M}i - \mathrm{O_F}i] \quad (6)$$

where the area of each package is limited to the overlapping region of the bounding horizons (e.g., Figure 6).

Mapping the Stratigraphic-Based Centroid Through Time

We also want to match the centroids $\bar{x}_{i,(1-4)}$ with the time span of preserved stratal accumulation. Of the four stratal terminations mapped, only $\mathrm{E_F}$ shows strong measurable diachroneity. To constrain time where this surface is involved, we incorporate linked surfaces $\mathrm{O_M}$ and $\mathrm{C_M}$. For example, each $\bar{x}_{i,1}$ is bracketed by $\mathrm{E_F}$ + $\mathrm{O_M}$ of the *i*th cycle and $\mathrm{D_M}$ of the *i*th – 1 cycle; $\bar{x}_{i,1}$ is then defined in time as the average temporal position between the two bounding time lines $\mathrm{D_{M}}i-1$ and $\mathrm{O_M}i$. This is done with the understanding that the kinematics of $\mathrm{E_F}$ formation impose a limit to the precision of matching strata to time. In this case, the evolution of $\mathrm{E_F}i$ indicates the potential for deposition above $\mathrm{E_F}i$ prior to $\mathrm{O_M}$ emplacement, but this strata cannot be included in formulating $\bar{x}_{i,1}$ using stratigraphic surfaces. The degree to which this is the case and the mechanistic controls on bypass versus fluvial retention during relative base-level fall are interesting for sequence stratigraphy and will be the focus of future work.

A similar imprecision exists for $\bar{x}_{i,2}$, where most, although not all, of the bounded strata between $\mathrm{E_F}i$ + $\mathrm{O_M}i$ and $\mathrm{E_F}i$ + $\mathrm{C_M}i$ were deposited between the time of $\mathrm{O_M}i$ formation and base-level minimum. The point $\bar{x}_{i,2}$ is positioned in time as the average time between the $\mathrm{O_M}i$ emplacement and base-level minimum.

In the case of $\bar{x}_{i,3}$, we account for diachronous $\mathrm{E_F}i$ formation by extending the lower bracket of sediment accumulation down the onset of relative base-level fall. In the time-space diagram in Figure 13, the result is coeval sedimentation below and above $\mathrm{E_F}$. The $\mathrm{O_F}i$ is bracketed in time by interpolating between neighboring topographic time lines. Based on topographic analysis, relative base-level fall sedimentation accounts for a relatively small volume fraction of the depositional unit in question. And although this is partially caused by data resolution, surface topography indicates that most of the accumulation between $\mathrm{E_F}i$ + $\mathrm{C_M}i$ and $\mathrm{O_F}i$ occurs after the time of base-level minimum. Consequently, we position $\bar{x}_{i,3}$ in time between base-level minimum and the interpolated time derived for $\mathrm{O_F}i$. The result is asymmetric uncertainty on the temporal location of $\bar{x}_{i,3}$ (Figure 13).

The point $\bar{x}_{i,4}$ is unrelated to $\mathrm{E_F}$ and is therefore relatively straightforward to evaluate: It is bracketed in time by finding the closest topographic time line to $\mathrm{D_M}i$, interpolating to find $\mathrm{O_F}i$, and then positioned by averaging.

Centroid Mapping Results

All depocenter results are shown in Figure 13, which shows two features worthy of note. First, despite imperfect mapping of the basinal stratigraphy, we observe close agreement between the mapped and known preserved depositional history. Second, both mass migration trajectories are in phase with, although basinward of, the shoreline. This first point supports sequence-stratigraphic horizons as robust indicators of mass balance. Moreover, they form mostly independently of the speed and details of the changing depositional

profile, both of which are unique for each stratigraphic cycle.

The consistent streamwise offset between preserved depositional mass and the shoreline is caused by marine sedimentation during base-level fall, which permits shoreline accretion basinward, and to two key preservation effects during base-level rise. First, much of base-level highstand deposition is subsequently eroded during the following base-level fall. This explains why both preserved depocenters are basinward of the shoreline during base-level rise, although shoreline transgression implies significant fluvial sediment impoundment. Another preservational effect is highlighted by the fact that commonly the stratigraphic-based centroid is situated basinward of the topographic-based centroid. The culprit is autogenic fluvial scour-and-fill processes, which obliterate stratigraphic horizons and severely limit their updip correlation. In a sequence-stratigraphic framework, autogenic fluvial processes act as a noisy filter, which can both destroy stratigraphic signals, such as the updip reaches of the O_F, E_F, and D_M, and obscure conceptual inferences, such as $E_F + C_M$ and O_M generation.

DISCUSSION

The above analysis highlights the benefit of applying interpretive skills developed within the sequence-stratigraphic method to a deposit where the answer is known. The most important result with respect to the field is that, when used as a tool to map and conceptualize sediment mass migration, the sequence-stratigraphic approach is reasonably robust (Figure 13).

The Sequence Stratigraphy of Experimental Strata

Using the depositional sequence model as our guide, two primary methods of interpreting the sequence stratigraphy of the XES 02 experimental strata clearly exist. Based on the original definition of Mitchum et al. (1977a), a basal sequence boundary appears to connect the erosional surface (our E_F) updip to the marine onlap surface on the slope (our $O_{M,W}$) and then ultimately to the correlative conformity of the onlap surface (Figure 14). An equally valid approach, however, is to interpret the E_F as the sequence boundary in its entirety and connect it to the C_M (or some average C_M position because it is not a through-going surface) (e.g., Van Wagoner et al., 1990; Van Wagoner, 1995) (Figure 14). Various methods to interpret the sequence boundary are presented by Catuneanu (2002), and our objective here is not to pass judgment on the two methods outlined here because they are both operationally useful. First, avoiding inherent bias in the data is simply very hard. We can easily imagine, for example, that the seismic expression of the sequence boundary would likely be $E_F + O_{M,W}$ because $O_{M,W}$ is readily observable. In outcrops, however, the sequence boundary would be more readily identified as $E_F + C_M$ because $O_{M,W}$ is typically low angle, mud prone, and poorly exposed. Second, we stress that, in XES 02, one could not interpret all of the stratigraphic cycles using either of these methods alone: in the slow cycle and src 5–6, the sequence boundary is only expressed as $E_F + C_M$ (recall that for these stratigraphic intervals no $O_{M,W}$ formed), whereas in src 1, the sequence boundary is only revealed by $E_F + O_{M,W}$ (here C_M cannot be identified because of erosion).

An important effect of dual sequence boundary correlation methods is that they can exist simultaneously: For the isolated rapid cycle and src 2–4, both methods of sequence boundary delineation are, for the most part, possible at the same location (Figure 14). Such an intriguing result demonstrates that diachronous surface evolution common to sediment-transporting systems and recorded in associated stratal surfaces can result in nonunique sequence boundary correlation. With this in mind, it is not surprising that strong spatiotemporal variability exists in sequence architecture.

The occurrence of coexisting sequence boundary correlation methods is not a scaling effect. More than anything, this configuration arises from relatively high preservation potential of the near-surface stratigraphy (although the forcing conditions are

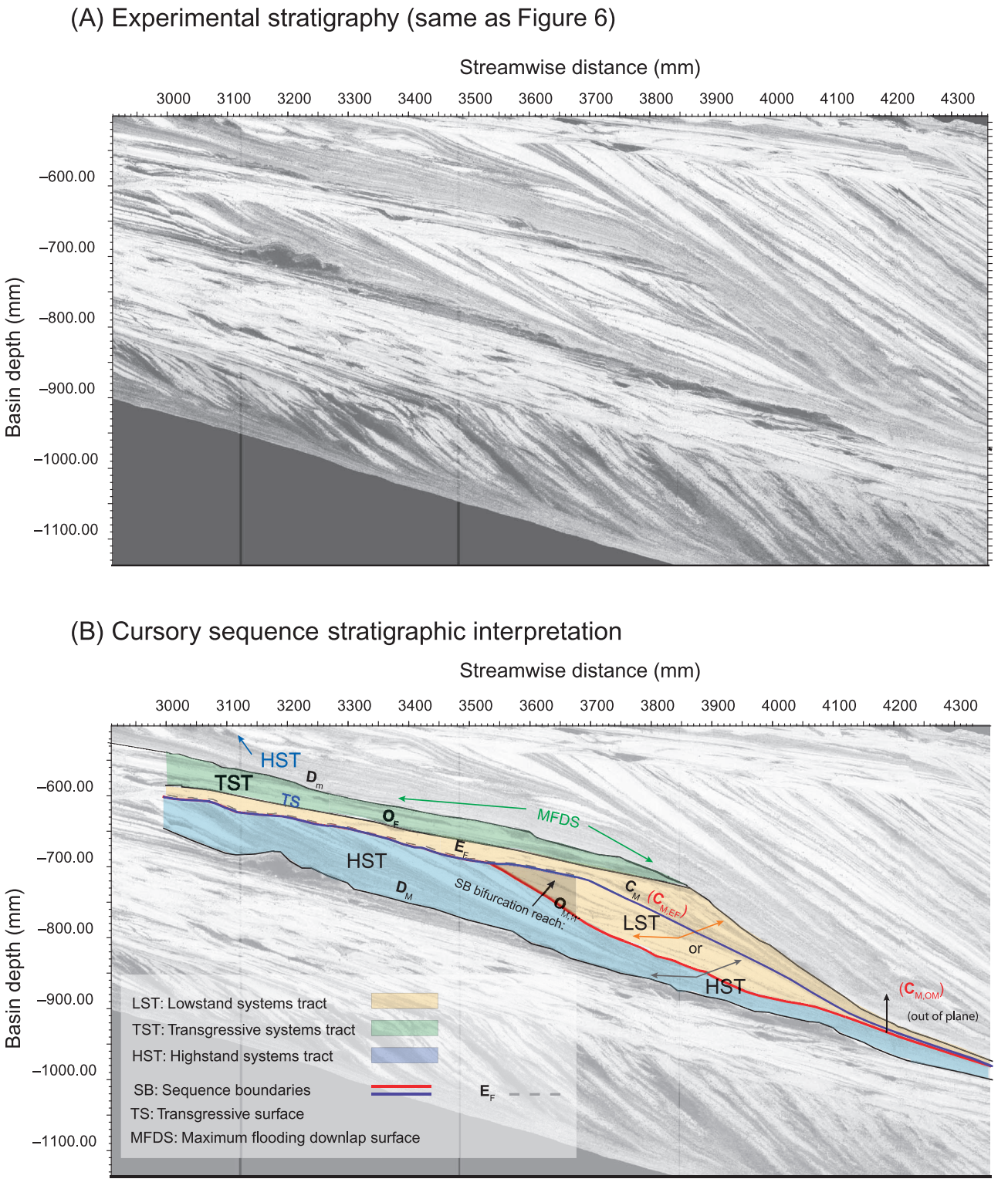

Figure 14. (A) Uninterpreted stratigraphic dip section at $y = 2300$ mm (90 in.) and (B) a cursory sequence-stratigraphic interpretation following the depositional sequence model. The two correlative conformities to the sequence boundary are (1) the correlative conformity to O_M, termed here $C_{M,OM}$, and (2) C_M, which to maintain consistency is termed $C_{M,EF}$. We use this nomenclature because it retains the physical relationships between the disconformable and conformable strata. The $C_{M,OM}$ is not physically present in this dip section; it is out of the plane and illustrates the strongly three-dimensional character of sediment accumulation and stratal stacking.

also important). And, terminology aside, the stratigraphic result is ultimately a more precise depositional record of sequence-stratigraphic accumulation. This is because the primary marine surfaces, $O_{M,W}$ and C_M, represent equally important records of change in the sediment mass balance. For example, $O_{M,W}$ and C_M are stratigraphic records of the approximate bound E_F evolution over its correlated area; that is, they record E_F diachroneity, and the correlative strata to E_F formation are bounded by $O_{M,W}$ and C_M. One potential use of these horizons is to partition the lowstand systems tract into a lower interval (bounded by $O_{M,W}$ and $E_F + C_M$) and an upper interval (bounded by $E_F + C_M$ and O_F). This issue is remarkably similar to previous work on falling-stage deposition (e.g., Hunt and Tucker, 1992; Posamentier et al., 1992; Plint and Nummedal, 2000). Although differences in formation processes exist, strata bounded by $O_{M,W}$ and $E_F + C_M$ are interpreted to be the functional equivalent of deposits variably linked to forced-regressive, falling-stage, or late highstand systems tracts (Catuneanu, 2002).

The departure from the depositional sequence model may be mostly caused by the inclusion of submarine canyons in the pioneering work on sequence-stratigraphic modeling (e.g., Posamentier et al., 1988; Van Wagoner et al., 1988), which act as sediment conduits that promote significant bypass along the sequence boundary. The bypass condition effectively stalls the basinward propagation of the subaerial part of the depositional sequence boundary and collapses $O_{M,W}$ and C_M to one surface. In contrast, basinward transfer of sediment in XES 02 occurs by clinoform accretion independent of the depositional profile (e.g., ramp versus shelf.). An interesting point worth some consideration is that $O_{M,W}$ does not necessarily imply longitudinal sediment bypass because it is readily produced from off-axis deposition.

The E_F and Stratigraphic Inference

The E_F evolution is not clear cut, and at a minimum, we can safely conclude that erosional etching of net depositional landscapes results in stratal discordances of uncertain chronostratigraphic significance. Sediment retention during base-level fall within incised valleys has been argued for several Quaternary systems and reflects a dynamically reasonable process for the creation of widespread erosional surfaces, such as subaerial sequence boundaries, based on diffusion considerations discussed above (Blum and Tornqvist, 2000). Another point of consideration is that increases in sediment flux are associated with increases in the frequency of topographic fluctuations. Sheets (2004) measured this relationship directly from experimental analysis, and Ashmore (1991) showed that higher sediment fluxes lead to increased channel mobility and greater confluence formation. The key morphodynamic relationship is that the transport system has the capacity to adjust itself to increased sediment flux, and greater confluence formation may indicate that transport becomes more efficient as supply increases (Paola, 2001). Incision associated with relative base-level fall results in significant increases in sediment flux, and we posit that this leads to more intensive fluvial scour-fill processes relative to other times in the base-level cycle. The positive relationship between flux and channel mobility suggests to us that local deposition may also increase because it is a primary mechanism to force channels to relocate laterally (Mohrig et al., 2000). The coupling between sediment flux and channel mobility likely contributes to the general pattern of downstream widening in incised valleys (e.g., Zaitlin et al., 1994; Strong and Paola, 2006). Additionally, we point out that more frequent (and perhaps greater magnitude) scouring and filling events are generally supported by the observation that all E_F in XES 02 are consistently well below all surface topography collected during their formation.

The indeterminate time significance of E_F, however, does not reduce its (or the subaerial part on the depositional sequence boundary's) (1) importance as a stratigraphic surface or (2) its gross value in reservoir prediction. After all, the sequence boundary was originally defined by discordant stratal contacts and not strictly as a time line (Mitchum et al., 1977a), and the refinements we

suggest above will in many cases be below seismic resolution. Instead, our finding represents a modification to the conceptual framework surrounding E_F that would be particularly important for reservoir-scale sequence analysis. At these scales, autogenic fluctuations in sediment transport can effectively decouple stratigraphic from individual topographic surfaces.

Future Work: Comparative Sequence Stratigraphy

Clearly, a succinct comparative study of sequence-stratigraphic models and the experimental stratigraphy outlined above would be helpful, primarily to address in more detail how observations here fit into the full range of previous work. Space does not permit this examination here, but we recognize three key outstanding issues that will be the focus of future work. First, relating the experimental stratal discordances to other sequence-stratigraphic models may be of value, especially given that concepts of the forcing effects on moving boundaries (e.g., the shoreline, depositional limits, etc.) and stratal formation are variable (e.g., Jervey, 1988; Posamentier and Vail, 1988; Nystuen, 1998; Catuneanu, 2002, 2006; Embry, 2002). Second, systems tract delineation, beyond being a natural outgrowth of comparative horizon analysis, may provide an additional perspective for various sequence-stratigraphic approaches because both stratigraphic and base-level perspectives can be evaluated (e.g., Galloway, 1989; Hunt and Tucker, 1992; Embry, 1993; Plint and Nummedal, 2000). Third, we submit that the stratigraphic sequence represents a superposition of readily apparent allogenic and autogenic depositional records (Muto et al., 2007). Although autogenic fluctuations are not particularly well constrained, recent work suggests that they are not limited to high-frequency noise and short length scales that can effectively be ignored in sequence-stratigraphic interpretation (e.g., Kim and Paola, 2007). The presence of multiple O_M is a good first example of this. Of interest for sequence stratigraphy is how internal and external forcings coevolve to produce and set the correlation limits of stratigraphic surfaces.

CONCLUSIONS

1. Mass-balance shifts driven by variable base level and linear differential subsidence, boundary conditions similar to those used in modern sequence stratigraphy, produce experimental stratigraphic discordances and packages similar to those observed in the field. Many basic sequence concepts appear to be independent of scale and of process details.
2. Allogenic-forced marine onlap surfaces ($O_{M,W}$) and marine downlap surfaces (D_M) demonstrate the closest time equivalence with instantaneous topographic horizons. This is because (1) both horizons, in most instances, represent relatively significant periods of nondeposition and (2) burial is mostly by passive deposition, two critical conditions for preserving original topography as depositional surfaces.
3. As such, $O_{M,W}$ and D_M are robust indicators of relative base-level fall and rise, respectively. The $O_{M,W}$ are especially useful because they exhibit the best preservation potential.
4. Autogenic-forced marine onlap patterns ($O_{M,L}$) produce multiple O_M and coexist with $O_{M,W}$. The distinguishing factor is the lateral persistence of O_M, where experimentally $O_{M,W}$ are expansive enough to produce one contiguous horizon, whereas $O_{M,L}$ are more precisely bundles of individual O_M that are laterally separated and cannot be correlated by a single horizon.
5. Subaerial erosional truncation surfaces (E_F) do not have a clear relation to any time line collected during base-level cycles. Relatively rapid erosion and deposition during base-level fall result in the E_F forming significantly lower (by up to three channel depths) than the topography at base-level minimums, which is the generally assumed instance of stratigraphic-geomorphic equivalence of widespread subaerial erosional surfaces, such as sequence boundaries. Topographic analysis reveals this by documenting sediment sequestration in the fluvial reach during base-level fall.
6. The stacking arrangement of stratigraphic packages (bounded by stratigraphic horizons) agrees closely with the known depositional history.

This shows that the mapped stratigraphic horizons are sensitive to the mass-balance configuration and form mostly independently of the rate of change of the depositional profile.

REFERENCES CITED

Ashmore, P., 1991, Channel morphology and bed load pulses in braided, gravel bed streams: Geografiska Annaler, v. 73A, p. 37–52, doi:10.2307/521212.

Blum, M. D., and A. Aslan, 2006, Signatures of climate vs. sea-level change within incised valley-fill successions: Quaternary examples from the Texas Gulf Coast: Sedimentary Geology, v. 190, p. 177–211, doi:10.1016/j.sedgeo.2006.05.024.

Blum, M. D., and T. E. Tornqvist, 2000, Fluvial responses to climate and sea-level changes: A review and look forward: Sedimentology, v. 47, suppl. 1, p. 2–48, doi:10.1046/j.1365-3091.2000.00008.x.

Blum, M. D., R. A. Morton, and J. M. Durbin, 1995, "Deweyville" terraces and deposits of the Texas Gulf coastal plain: Transactions of the Gulf Coast Association of the Geological Society, v. 45, p. 53–60.

Blum, M. D., M. J. Guccione, D. A. Wysocki, and P. C. Robnett, 2000, Late Pleistocene evolution of the central Mississippi Valley, southern Missouri to Arkansas: Geological Society of America Bulletin, v. 112, p. 221–235, doi:10.1130/0016-7606(2000)112<0221:LPEOTL>2.3.CO;2.

Catuneanu, O., 2002, Sequence stratigraphy of clastic systems: Concepts, merits, and pitfalls: Journal of African Earth Sciences, v. 35, p. 1–43, doi:10.1016/S0899-5362(02)00004-0.

Catuneanu, O., 2006, Principles of sequence stratigraphy: Amsterdam, Elsevier, 336 p.

Catuneanu, O., A. Willis, and A. D. Miall, 1998, Temporal significance of sequence boundaries: Sedimentary Geology, v. 47, p. 157–178, doi:10.1016/S0037-0738(98)00084-0.

Cross, T. A., and M. A. Lessenger, 1998, Sediment volume partitioning: Rationale for stratigraphic model evaluation and high-resolution stratigraphic correlation, *in* F. M. Gradstein, K. O. Sandvik, and N. J. Milton, eds., Sequence stratigraphy: Concepts and applications: Norwegian Petroleum Society Special Publication 8, p. 171–196.

Crowley, T., and G. R. North, 1991, Paleoclimatology: New York, Oxford University Press, 360 p.

Edmonds, D. A., D. C. Hoyal, B. Sheets, and R. B. Bloch, 2007, On the nature of delta distributary fill (abs.): AAPG Annual Meeting Abstracts, v. 16, p. 40.

Embry, A. F., 1993, Transgressive-regressive (T-R) sequence analysis of the Jurassic succession of the Sverdrup Basin, Canadian Arctic Archipelago: Canadian Journal of Earth Science, v. 30, p. 301–320.

Embry, A. F., 2001, The six surfaces of sequence stratigraphy: AAPG Hedberg Research Conference on Sequence Stratigraphic and Allostratigraphic Principles and Concepts, Dallas, August 26–29, Program and Abstracts Volume, p. 26–27.

Embry, A. F., 2002, Transgressive-regressive (T-R) sequence stratigraphy, *in* J. Armentrout and N. Rosen, eds., Sequence stratigraphic models for exploration and production: Evolving methodology, emerging models, and application histories, proceedings: Gulf Coast Association of Geological Societies Transactions 52, p. 151–172.

Foufoula-Georgiou, E., and V. B. Sapazhnikov, 1998, Anisotropic scaling in braided rivers: An integrated theoretical framework and results from application to an experimental river: Water Resources Research, v. 34, p. 863–867, doi:10.1029/98WR00216.

Foufoula-Georgiou, E., and V. B. Sapazhnikov, 2001, Scale invariances in the morphology and evolution of braided rivers: Mathematical Geology, v. 33, p. 273–291, doi:10.1023/A:1007682005786.

Frasier, D. E., 1974, Depositional episodes: Their relationship to the Quaternary stratigraphic framework in the northwestern portion of the Gulf Basin: University of Texas at Austin, Bureau of Economic Geology Geological Circular, v. 4, no. 1, 28 p.

Galloway, W. E., 1989, Genetic stratigraphic sequences in basin analysis: Architecture and genesis of flooding surface bounded depositional units: AAPG Bulletin, v. 73, p. 125–142.

Goldhammer,R. K., P. A. Dunn, and L. A. Hardie, 1987, High-frequency glacio-eustatic sea-level oscillatins with Milankovitch characteristics recorded in Middle Triassic platform carbonates in northern Italy: American Journal of Science, v. 287, p. 853–892.

Haq, B. U., J. Hardenbol, and P. R. Vail, 1987, Chronology of fluctuating sea levels since the Triassic: Science, v. 235, p. 1153–1165.

Hasbargen, L. E., and C. Paola, 2000, Landscape instability in an experimental drainage basin: Geology, v. 28, p. 1067–1070, doi:10.1130/0091-7613(2000)28<1067:LIIAED>2.0.CO;2.

Helland-Hanson, W., and J. G. Gjelberg, 1994, Conceptual basis and variability in sequence stratigraphy: A different perspective: Sedimentary Geology, v. 92, p. 31–52, doi:10.1016/0037-0738(94)90053-1.

Helland-Hanson, W., and O. J. Martinson, 1996, Shoreline trajectories and sequences: Description of variable depositional dip scenarios: Journal of Sedimentary Research, v. 66, no. 4., p. 670–688.

Hickson, T. A., B. A. Sheets, C. Paola, and M. Kelberer, 2005, Experimental test of tectonic controls on three-dimensional alluvial facies architecture: Journal of Sedimentary Research, v. 75, p. 710–722, doi:10.2110/jsr.2005.057.

Hooke, R. L., 1968, Model geology: Prototype and laboratory streams: Discussion: Geological Society of America Bulletin, v. 79, p. 391–394, doi:10.1130/0016-7606(1968)79[391:MGPALS]2.0.CO;2.

Hoyal, D. C. J. D., and B. A. Sheets, in press, Morphodynamic evolution of experimental deltas: Journal of Geophysical Research-Earth Surface, doi:10.1029/2007;f000882.

Hunt, D., and M. E. Tucker, 1992, Stranded parasequences and the forced regressive wedge systems tract: Deposition

during base-level fall: Sedimentary Geology, v. 81, p. 1–9, doi:10.1016/0037-0738(92)90052-S.
Jervey, M. T., 1988, Quantitative geological modeling of siliciclastic rock sequences and their seismic expressions, *in* C. K. Wilgus, B. S. Hastings, C. G. St. C. Kendall, H. W. Posamentier, C. A. Ross, and J. C. Van Wagoner, eds., Sea-level changes: An integrated approach: SEPM Special Publication 42, p. 47–69.
Jones, R. W., and N. J. Milton, 1994, Sequence development during uplift: Paleogene stratigraphy and relative sea level history of the Ourter Moray Firth, United Kingdom North Sea: Marine Petroleum Geology, v. 11, p. 57–165.
Kendall, C. G. St. C., J. Strobel, R. Cannon, J. Bezdek, and G. Biswas, 1991, The simulation of the sedimentary fill of basins: Journal of Geophysical Research, v. 96, p. 6911–6929, doi:10.1029/90JB01406.
Kim, W., and T. Muto, 2007, Autogenic response of alluvial-bedrock transition to base-level variation: Experiment and theory: Journal of Geophysical Research-Earth Surface, v. 112, F04S14, doi:10.1029/2006JF000561.
Kim, W., and C. Paola, 2007, Long-period cyclic sedimentation with constant tectonic forcing in an experimental relay ramp: Geology, v. 35, p. 331–334, doi:10.1130/G23194A.1.
Kim, W., C. Paola, V. R. Voller, and J. B. Swenson, 2006, Experimental measurement of the relative importance of controls on shoreline migration: Journal of Sedimentary Research, v. 76, no. 2, p. 270–283, doi:10.2110/jsr.2006.019.
Lawrence, D. T., 1994, Evaluation of eustasy, subsidence, and sediment input as controls on depositional sequence geometries and the synchroneity of sequence boundaries, *in* P. Weimer and H. W. Posamentier, eds., Siliciclastic sequence stratigraphy: recent developments and applications: AAPG Memoir 58, p. 337–367.
Massey, B. S., 1989, Mechanics of fluids: United Kingdom, Taylor and Francis, 628 p.
Mitchum, R. M., 1985, Seismic stratigraphic expression of submarine fans, *in* O. R. Berg and D. G. Woolverton eds., Seismic stratigraphy: II. An integrated approach to hydrocarbon exploration: AAPG Memoir 39, p. 117–136.
Mitchum, R. M., and J. C. Van Wagoner, 1991, High-frequency sequences and their stacking patterns, sequence stratigraphic evidence of high-frequency eustatic cycles: Sedimentary Geology, v. 70, p. 131–160, doi:10.1016/0037-0738(91)90139-5.
Mitchum Jr., R. M., P. R. Vail, and S. Thompson III, 1977a, Seismic stratigraphy and global changes of sea-level: Part 2. The depositional sequence as a basic unit for stratigraphic analysis, *in* C. E. Payton, ed., Seismic stratigraphy—Applications to hydrocarbon exploration: AAPG Memoir 26, p. 53–62.
Mitchum, R. M., P. R. Vail, and J. B. Sangree, 1977b, Seismic stratigraphy and global changes of sea level: Part 6. Stratigraphic interpretation of seismic reflection patterns in depositional sequences, *in* C. E. Payton, ed., Seismic stratigraphy—Applications to hydrocarbon exploration: AAPG Memoir 26, p. 117–133.
Mohrig, D., P. L. Heller, C. Paola, and W. J. Lyons, 2000, Interpreting avulsion process from ancient alluvial sequences: Guadalope-Matarranya system (northern Spain) and Wasatch Formation (western Colorado): Geological Society of America Bulletin, v. 112, no. 12, p. 1787–1803, doi:10.1130/0016-7606(2000)112<1787:IAPFAA>2.0.CO;2.
Mullin, J., and C. Ellis, 2008, Method to produce grain-scale digital images of large experimental sedimentary deposits and other imperfectly flat stratigraphy: Journal of Sedimentary Research, v. 78, p. 239–244, doi:10.2110/jsr.2008.024.
Muto, T., and R. J. Steel, 2001, Autostepping during the transgressive growth of deltas: Results from flume experiments: Geology, v. 29, no. 9, p. 771–774, doi:10.1130/0091-7613(2001)029<0771:ADTTGO>2.0.CO;2.
Muto, T., R. J. Steel, and J. B. Swenson, 2007, Autostratigraphy: A framework norm for genetic stratigraphy: Journal of Sedimentary Research, v. 77, p. 2–12, doi:10.2110/jsr.2007.005.
Nystuen, J. P., 1998, History and development of sequence stratigraphy, *in* F. M. Gradstein, K. O. Sandvik, and N. J. Milton, eds., Sequence stratigraphy: Concepts and applications: Norwegian Petroleum Society Special Publication 8, p. 31–116.
Paola, C., 2000, Quantitative models of basin filling: Sedimentology, v. 47, suppl. 1, p. 121–178, doi:10.1046/j.1365-3091.2000.00006.x.
Paola, C., 2001, Modeling stream braiding over a range of scales, *in* M. P. Mosley, ed., Gravel bed rivers V: Wellington, New Zealand Hydrological Society, p. 11–45.
Paola, C., P. L. Heller, and C. L. Angevine, 1992, The large-scale dynamics of grain-size variation in alluvial basins: 1. Theory: Basin Research, v. 4., p. 73–90.
Paola, C., et al., 2001, Experimental stratigraphy: GSA Today, v. 11, p. 4–9, doi:10.1130/1052-5173(2001)011<0004:ES>2.0.CO;2.
Peakall, J., P. Ashworth, and J. Best, 1996, Physical modeling in fluvial geomorphology: Principles, applications, and unresolved issues, *in* B. L. Rhoads and C. E. Thorn, eds., The scientific nature of geomorphology: Chichester, John Wiley & Sons, p. 221–253.
Perlmutter, M. A., B. J. Radovich, M. D. Matthews, and C. G. St. C. Kendall, 1998, The impact of high-frequency sedimentation cycles on stratigraphic interpretation, *in* F. M. Gradstein, K. O. Sandvik, and N. J. Milton, eds., Sequence stratigraphy: Concepts and applications: Norwegian Petroleum Society Special Publication 8, p. 141–170.
Plint, A. G., and D. Nummedal, 2000, The falling stage systems tract: Recognition and importance in sequence stratigraphic analysis, *in* D. Hunt and R. Gawthorpe, eds., Sedimentary responses to forced regressions: Geological Society of London Special Publication 172, p. 1–17.
Posamentier, H. W., and P. R. Vail, 1988, Eustatic controls on clastic deposition: I. Sequence and systems tract models, *in* C. K. Wilgus, B. S. Hastings, C. G. St. C. Kendall, H. W. Posamentier, C. A. Ross, and J. C. Van Wagoner, eds., Sea-level changes: An integrated approach: SEPM Special Publication 42, p. 109–124.
Posamentier, H. W., M. T. Jervey, and P. R. Vail, 1988, Eustatic controls on clastic deposition: II. Conceptual

framework, *in* C. K. Wilgus, B. S. Hastings, C. G. St. C. Kendall, H. W. Posamentier, C. A. Ross, and J. C. Van Wagoner, eds., Sea-level changes: An integrated approach: SEPM Special Publication 42, p. 125–154.

Posamentier, H. W., G. P. Allen, D. P. James, and M. Tesson, 1992, Forced regressions in a sequence stratigraphic framework: Concepts, examples and exploration significance: AAPG Bulletin, v. 76, p. 1687–1709.

Rodriguez-Iturbe, I., and A. Rinaldo, 1997, Fractal river basins: Chance and self-organization: Cambridge, United Kingdom, Cambridge University Press, 547 p.

Sapozhnikov, V. B., and E. Foufoula-Georgiou, 1996, Self-affinity in braided rivers: Water Resources Research, v. 32, p. 1429–1439, doi:10.1029/96WR00490.

Schlager, W., 2004, Fractal nature of stratigraphic sequences: Geology, v. 32, no. 3, p. 185–188.

Sheets, B., 2004, Assembling the stratigraphic record: Depositional patterns and time-scales: Ph.D. dissertation, University of Minnesota, 123 p.

Sheets, B., T. Hickson, and C. Paola, 2002, Assembling the stratigraphic record: Depositional patterns and time-scales in an experimental alluvial basin: Basin Research, v. 14, p. 287–301, doi:10.1046/j.1365-2117.2002.00185.x.

Strong, N., and C. Paola, 2006, Fluvial landscapes and stratigraphy in a flume: The Sedimentary Record, v. 4, no. 2, p. 4–8.

Strong, N., and C. Paola, 2008, Valleys that never were: Time surfaces versus stratigraphic surfaces: Journal of Sedimentary Research, v. 78, p. 579–593, doi:10.2110/jsr.2008.059.

Tornqvist, T. E., J. Wallinga, and F. S. Busschers, 2003, Timing of the last sequence boundary in a fluvial setting near the highstand shoreline—Insights from optical dating: Geology, v. 31, no. 3, p. 279–282, doi:10.1130/0091-7613(2003)031<0279:TOTLSB>2.0.CO;2.

Vail, P. R., R. M. Mitchum, and S. Thompson III, 1977, Seismic stratigraphy and global changes of sea-level: Part 3. Relative changes of sea level from coastal onlap, *in* C. E. Payton, ed., Seismic stratigraphy—Applications to hydrocarbon exploration: AAPG Memoir 26, p. 63–82.

Van Heijst, M. W. I. M., and G. Postma, 2001, Fluvial response to sea-level changes: A quantitative analog, experimental approach: Basin Research, v. 13, p. 269–292, doi:10.1046/j.1365-2117.2001.00149.x.

Van Wagoner, J. C., 1995, Sequence stratigraphy and marine to nonmarine facies architecture of foreland basin strata, Book Cliffs, Utah, U.S.A, *in* J. C. Van Wagoner and G. T. Bertram, eds., Sequence stratigraphy of foreland basin deposits: AAPG Memoir 64, p. 137–224.

Van Wagoner, J. C., H. W. Posamentier, R. M. Mitchum, P. R. Vail, J. F. Sarg, T. S. Loutit, and J. Hardenbol, 1988, An overview of the fundamentals of sequence stratigraphy and key definitions, *in* C. K. Wilgus, B. S. Hastings, C. G. St. C. Kendall, H. W. Posamentier, C. A. Ross, and J. C. Van Wagoner, eds., Sea-level changes: An integrated approach: SEPM Special Publication 42, p. 39–45.

Van Wagoner, J. C., R. M. Mitchum, K. M. Campion, and V. D. Rahmanian, 1990, Siliciclastic sequence stratigraphy in well logs, cores, and outcrops: Concepts for high-resolution correlation of time and facies: AAPG Methods in Exploration 7, 55 p.

Wheeler, H. E., 1958, Time-stratigraphy: AAPG Bulletin, v. 42, p. 1047–1063.

Zaitlin, B., R. W. Dalrymple, and R. Boyd, 1994, The stratigraphic organization of incised-valley systems, *in* R. W. Dalrymple, R. Boyd, and B. Zaitlin, eds., Incised-valley systems: Origin and sedimentary sequences: Society for Sedimentary Geology Special Publication 51, p. 45–60.